JPn Neuroscience
The Journal of Physiology

J Physiol 593.1 (2015) pp 161–180

$GABA_B$ receptor-mediated tonic inhibition regulates the spontaneous firing of locus coeruleus neurons in developing rats and in citalopram-treated rats

Han-Ying Wang[1,2], Zhao-Chen Kuo[2], Yu-Show Fu[6], Ruei-Feng Chen[1,2,3], Ming-Yuan Min[1,2,3] and Hsiu-Wen Yang[4,5]

[1] *Institute of Zoology, National Taiwan University, Taipei 107, Taiwan*
[2] *Department of Life Science, National Taiwan University, Taipei 107, Taiwan*
[3] *Center for Neurobiology and Cognition Science, National Taiwan University, Taipei 107, Taiwan*
[4] *Department of Biomedical Sciences, Chung Shan Medical University, Taichung 402, Taiwan*
[5] *Department of Medical Research, Chung Shan Medical University, Taichung 402, Taiwan*
[6] *Department of Anatomy and Cell Biology, National Yang-Ming University, Taipei 112, Taiwan*

Key points

- Noradrenaline (NA)-releasing neurons in the locus coeruleus (LC) provide NA to the forebrain and play important roles in regulating many brain functions.
- LC neurons are subject to tonic inhibition mediated by $GABA_B$ receptors ($GABA_B$Rs) and that the extent of the effect varies with ambient GABA levels.
- $GABA_B$R-mediated tonic inhibition can effectively tune the spontaneous firing rate (SFR) of LC neurons; it is developmentally regulated and is responsible for maintaining a constant SFR of LC neurons during development.
- In male, but not female rats, chronic perinatal treatment with citalopram, a selective serotonin reuptake inhibitor, results in downregulation of $GABA_B$R-mediated tonic inhibition of LC neurons that partially accounts for increased SFR in male, but not female, rats receiving such treatment.
- Our results show that $GABA_B$R-mediated tonic inhibition could be an important player in the development of normal and abnormal behaviours/brain functions associated with the LC–NA system.

Abstract Noradrenaline (NA)-releasing neurons in the locus coeruleus (LC) provide NA to the forebrain. Their activity is believed to be a key factor regulating the wakefulness/arousal level of the brain. In this study, we found that the activity of NA-releasing neurons in the LC (LC neurons) was subject to γ-aminobutyric acid (GABA) tonic inhibition through $GABA_B$ receptors ($GABA_B$Rs), but not $GABA_A$ receptors. The intensity of $GABA_B$R tonic inhibition was found to depend on ambient GABA levels, as it was dramatically increased by blockade of GABA reuptake. It also varied with the function of $GABA_B$Rs. The $GABA_B$R activity on LC neurons was found to increase with postnatal age up to postnatal days 8–10, resulting in increased tonic inhibition. Interestingly, there was no significant difference in the spontaneous activity of LC neurons at different postnatal ages unless $GABA_B$R tonic inhibition was blocked. These results show that, during postnatal development, there is a continuous increase in $GABA_B$R tonic inhibition that maintains the activity of LC neurons at a proper level. In male, but not female, rats, chronic perinatal treatment with citalopram, a selective serotonin reuptake inhibitor, reduced $GABA_B$R activity and tonic inhibition, which might result in the significantly higher spontaneous activity of LC neurons seen in these animals. In conclusion, our results show that $GABA_B$R-mediated tonic inhibition has a direct impact on the spontaneous activity of LC neurons and that the extent of the effect varies with ambient GABA levels and functionality of $GABA_B$R signalling.

DOI: 10.1113/jphysiol.2014.281378

(Resubmitted 24 July 2014; accepted after revision 30 September 2014; first published online 17 October 2014)
Corresponding authors H.-W. Yang: Department of Biomedical Sciences, Chung Shan Medical University, 110, Chien-Kuo N. Rd, Sec. 1, Taichung 402, Taiwan. Email: hwy@csmu.edu.tw; R.-F. Chen: Email: rfchen@ntu.edu.tw; M.-Y. Min: Email: mymin@ntu.edu.tw

Abbreviations ACSF, artificial cerebrospinal fluid; AP, action potential; a2AR, a2-adrenoreceptor; BicmBr, bicuculline methobromine; CBX, carbenoxolone; CTM, citalopram; EM, electron microscopy; GABA, γ-aminobutyric acid; $GABA_AR$, $GABA_A$ receptor; $GABA_BR$, $GABA_B$ receptor; GAT, GABA transporter; GBZ, gabazine; GIRK, G protein-coupled inwardly-rectifying potassium channel; $5\text{-}HT_{1A}R$, $5\text{-}HT_{1A}$ receptor; I_{GABA}, GABA-induced whole-cell current; I_{Bac}, baclofen-induced whole-cell current; $I_{Bac\text{-}Max}$, the maximal I_{Bac}; $I_{GABA\text{-}Max}$, the maximal I_{GABA}; IHC, immunohistochemistry; IPSCs, inhibitory postsynaptic currents; ir, immunoreactive; I_{Stand}, standing current; LC, locus coeruleus; mIPSCs, miniature IPSCs; NA, noradrenaline; PB, phosphate buffer; PBS, phosphate-buffered saline; PBST, PBS containing 0.03% Triton X-100; PN, postnatal day; REM, rapid eye movement; SFR, spontaneous firing rate; SSRI, selective serotonin reuptake inhibitor; TH, hydroxylase; TTX, tetrodotoxin; V_m, membrane potential.

Introduction

Noradrenaline (NA) plays important roles in regulating many brain functions (Aston-Jones & Cohen, 2005; Tully & Bolshakov, 2010; Berridge *et al.* 2012). The major NA supply to the forebrain is from NA-releasing neurons in the locus coeruleus (LC), which is located in the dorsal pontine area. The NA-releasing neurons in the LC (referred to as LC neurons hereafter) spontaneously fire action potentials (APs) in a brain state-dependent manner (Aston-Jones & Cohen, 2005), displaying active firing during wakefulness and a decreased discharge rate during non-rapid eye movement (non-REM) sleep, and being silent during REM sleep. Since pharmacological activation or inhibition of their activity is always followed by a change in forebrain electroencephalographic activity, LC neurons are believed to control the wakefulness/arousal level of the brain (Adam & Foote, 1988; Berridge & Foote, 1991).

Several lines of evidence suggest that γ-aminobutyric acid (GABA), the principal inhibitory neurotransmitter in the brain, is involved in regulating LC neuron activity. Somogyi & Llewellyn-Smith (2001) showed that about two-thirds of synapses on LC neurons are GABAergic, while other studies showed that a substantial proportion of these GABAergic inputs come from the sleep-promoting nuclei, such as the ventrolateral preoptic nucleus (Lu *et al.* 2002; Luppi *et al.* 2006). Moreover, ambient GABA levels in the LC are significantly higher during REM/non-REM sleep than during wakefulness (Nitz & Siegel, 1997; Nelson *et al.* 2002). GABA, which acts on ionotropic $GABA_A$ receptors ($GABA_ARs$) and metabotropic $GABA_B$ receptors ($GABA_BRs$), provides important inhibitory control of neuronal circuits in the brain. In addition to classic phasic inhibition, $GABA_ARs$ with a high affinity for GABA and extrasynaptic or perisynaptic location, are continuously activated by ambient GABA, thereby mediating a tonic inhibition that allows the long-term regulation of neuronal excitability (Farrant & Nusser, 2005). Tonic inhibition mediated by $GABA_ARs$ has been reported throughout the brain and identified as an important player in both physiological and pathophysiological processes (Glykys & Mody, 2007*a*; Belelli *et al.* 2009).

Interestingly, recent reports have shown that GABA tonic inhibition in A6 (the LC) and A7 catecholamine cells in the pons (Wu *et al.* 2011; Wang *et al.* 2012) and layer 2/3 pyramidal neurons in the medial prefrontal cortex (Wang *et al.* 2010) is mediated by $GABA_BRs$, but not $GABA_ARs$. Since GABA is important for regulating LC neuron activity, the aims of the present study were to fully characterize the $GABA_BR$-mediated tonic inhibition of LC neurons and determine the functional outcome of manipulations that increase or decrease it. In brainstem neurons $GABA_BR$ activity is reported to increase during development (Pfeiffer & Zhang, 2007) and to be reduced in animals receiving chronic treatment with a selective serotonin reuptake inhibitor (SSRI) (Cornelisse *et al.* 2007). In our study, normal postnatal development and chronic perinatal treatment with citalopram (CTM), a SSRI, were therefore used as study models for an increase or reduction in $GABA_BR$ tonic inhibition, respectively. Our results showed that $GABA_BR$-mediated GABA tonic inhibition is developmentally regulated and is responsible for maintaining a constant spontaneous firing rate (SFR) of LC neurons. In male, but not female rats, chronic perinatal treatment with CTM resulted in downregulation of $GABA_BR$-mediated tonic inhibition of LC neurons, which partially accounts for the phenomenon reported by Darling *et al.* (2011), who used the same chronic perinatal CTM treatment procedures as ourselves and showed that the SFR of LC neurons is increased in male, but not female, rats receiving such treatment.

Methods

Animals

All animal experiments complied with the European Communities Council Directive (24 November 1986), and the use of animals in this study was approved by the

Ethics Committee for Animal Research of National Taiwan University and Chung Shan Medical University. Every effort was made to minimize the number of animals used and their suffering. Sprague–Dawley rat pups of both sexes were used and were killed for slice preparation on postnatal day (PN) 8–10 in all electrophysiology experiments except the developmental study and the CTM treatment study. In the developmental study, rats were killed on PN2–4, PN8–10 and PN18–20, while, in the CTM treatment study, they were injected subcutaneously with CTM (10 mg (kg body weight)$^{-1}$) or 0.9% NaCl (controls) twice a day for 7 days, starting on PN5, and were killed on PN18–20. For characterization of $GABA_B$R-mediated tonic inhibition (Figs 1, 2, 4 and 5) and the developmental study (Fig. 6), 14 PN2–4, 29 PN8–10 and 17 PN18–20 rats were used, and for the CTM treatment study (Figs 7 and 8) 21 male and 19 female rats were used. Another three naive rats (Fig. 3), and three saline-treated and three CTM-treated male rats (Fig. 9) were used for electron microscopy (EM) study.

Preparation of brainstem slices and electrophysiology

The animals were anaesthetized with 5% isoflurane in O_2 and decapitated, then their brains were rapidly exposed and chilled with ice-cold artificial cerebrospinal fluid (ACSF) consisting of (in mM): 119 NaCl, 2.5 KCl, 1.3 $MgSO_4$, 26.2 $NaHCO_3$, 1 NaH_2PO_4, 2.5 $CaCl_2$ and 11 glucose, oxygenated with 95% O_2 and 5% CO_2, pH 7.4. Sagittal brainstem slices (300 μm) containing the LC were prepared using a vibroslicer (D.S.K. Super Microslicer Zero 1, Dosaka EM, Kyoto, Japan) and were maintained in a moist air–liquid (ACSF) interface chamber and allowed to recover for at least 90 min before being transferred to an immersion-type chamber mounted on an upright microscope (BX51WI, Olympus Optical Co., Ltd, Tokyo, Japan) for recording. Throughout the recording period, they were perfused at 2–3 ml min^{-1} with oxygenated ACSF containing 5 mM kynurenic acid (or a combination of 10 μM DNQX and 50 μM APV) and 1 μM strychnine to block glutamatergic and glycinergic synaptic transmission, respectively. The 'baseline recordings' described in this paper refer to the recordings made under these conditions unless noted otherwise.

Neurons were viewed using Nomarski optics. Patch pipettes were pulled from borosilicate glass tubing (1.5 mm outer diameter, 0.32 mm wall thickness; Warner Instruments Corp., Hamden, CT, USA) and had a resistance of about 3–5 MΩ when filled with the pipette solutions. To record the $GABA_B$R-mediated current, the pipette solution consisted of (in mM): 131 potassium gluconate, 20 KCl, 10 Hepes, 2 EGTA, 8 NaCl, 2 ATP, and 0.3 GTP, pH adjusted to 7.2 with KOH. To record the $GABA_A$R-mediated current, the potassium gluconate was replaced with an equimolar concentration of CsCl. To record the inhibitory postsynaptic currents (IPSCs), the potassium gluconate was replaced with an equimolar concentration of KCl. Recordings were made at 33°C in either the cell-attached or whole-cell configuration with a patch amplifier (Multiclamp 700B; Axon Instruments Inc., Union City, CA, USA). For current-clamp recording, the bridge was balanced and recordings were only accepted if the recorded neuron had a membrane potential (V_m) of at least –45 mV without applying a holding current and if the AP was able to overshoot 0 mV. For voltage-clamp recording in the whole-cell configuration, neurons were clamped at –70 mV unless specified otherwise. The series resistance was monitored throughout recording and the data discarded if the values varied by more than 20% of the original value, which was usually less than 20 MΩ. For recording in the cell-attached configuration, the holding current was set to 0 pA so that the recorded neurons were at their resting membrane potential during recording. Extracellular stimulation was performed by delivering a stimulating train through a bipolar stainless steel electrode (FHC, Bowdoinham, ME, USA) positioned in the LC. The stimulating train consisted of five constant-current pulses (50–250 μA; 100 μs) at 50 Hz and was delivered every 30 s. Signals were low-pass filtered at a corner frequency of 2 kHz and digitized at 10 kHz using a Micro 1401 interface running Signal software for episode-based capture or Spike2 software for continuous recording (Cambridge Electronic Design, Cambridge, UK). The miniature IPSCs were recorded with the addition of 1 μM tetrodotoxin (TTX) into the bath and were measured and analysed using the Mini-Analysis program (Synaptosoft Inc., Fort Lee, NJ, USA). The measurement of $GABA_A$R tonic current or $GABA_B$R standing current was modified from that described by Glykys & Mody (2007*b*). Briefly, the entire digitized recording was loaded and seal tests were removed from the traces. An all-point histogram was plotted for every 10,000 points. A Gaussian was fitted to the distribution, and the mean and standard deviation of the fitted Gaussian were considered to be the mean holding current and the noise level, respectively. This process was repeated for the entire recording and all baseline mean values were obtained. A segment of the baseline data was plotted and a linear fit was obtained and extended to the whole recording to correct for potential steady shifts during the recordings. A period of 30 s was used for the baseline and in the presence of drugs (bicuculline methiodide or CGP54626). The magnitude of tonic or standing current was obtained by subtracting the baseline current recorded in the presence of the drugs. All data are presented as the mean ± standard error of the mean (SEM) and were compared using Student's *t* test, the paired *t* test, one-way ANOVA, or two-way ANOVA. Bonferroni's *post hoc* test was used for selected pairwise comparisons when significant group-dependent differences were

observed. The criterion for significance was a P value < 0.05.

All chemicals used to prepare the ACSF and pipette solution, and $BaCl_2$ and paraformaldehyde, were from Merck (Frankfurt, Germany), baclofen, biocytin, carbenoxolone (CBX), kynurenic acid, and strychnine were from Sigma (St Louis, MO, USA), and DL-2-amino-5-phosphonopentanoic acid (APV), bicuculline methobromine (BicmBr), CGP35348, CGP54626 hydrochloride, 6,7-dinitroquinoxaline-2,3-dione (DNQX), gabazine (GBZ), NNC711, SCH50911, (s)-SNAP 5114, and tetrodotoxin (TTX) were from Tocris Cookson (Bristol, UK).

Biocytin histochemistry and immunohistochemistry (IHC)

In some experiments, 6.7 mM biocytin was included in the internal solution to fill the recorded neurons. The detailed procedures for viewing the biocytin-filled neurons and *post hoc* immunohistochemistry (IHC) for cell-type identification have been described previously (Min *et al.* 2008). Briefly, after recording, the slices were fixed overnight at 4°C in 4% paraformaldehyde in 0.1 M phosphate buffer (PB), pH 7.4, then were subjected to biocytin histochemistry and IHC procedures without further sectioning. The slices were incubated for 1 h at room temperature in phosphate-buffered saline (PBS) containing 0.03% Triton X-100 (PBST), 2% bovine serum albumin, and 10% normal goat serum, then were incubated overnight at 4°C in PBST containing a 1/1300 dilution of rabbit antibodies against tyrosine hydroxylase (TH) (Merck Millipore, cat. no. AB5986P, Darmstadt, Germany) and a 1/200 dilution of avidin-AMCA (Vector Laboratories, Burlingame, CA, USA). After PBST rinses, they were incubated for 2 h with a 1/50 dilution in PBST of tetramethylrhodamine isothiocyanate-conjugated goat anti-rabbit IgG antibodies (Jackson ImmunoResearch, West Grove, PA, USA), then observed under a fluorescence microscope (Axioplan 2, Zeiss, Oberkochen, Germany) or a confocal microscope (Leica TCS SP5, Hamburger, Germany).

$GABA_BR$ immunohistochemistry for electron microscopy (EM)

Animals were deeply anaesthetized with sodium pentobarbitone and perfused via the cardiovascular system with normal saline, followed by 4% paraformaldehyde and 0.1% glutaraldehyde in 0.1 M PB. The pre-embedding IHC method was used. Sagittal LC sections (70 μm thick) were cut with a Vibratome (Ted Pella, Inc., Redding, CA, USA) and equilibrated in cryoprotectant solution consisting of 25% sucrose and 10% glycerol in 0.05 M PB. To enhance the tissue penetration of reagents, the sections were freeze-thawed by freezing in liquid nitrogen-cooled isopentane, followed by liquid nitrogen, and thawed in PBS. The sections were preincubated for 1 h in PBS containing 2% bovine serum albumin and 10% normal goat serum, then for 48 h at 4°C with guinea pig anti-$GABA_BR1_{A/B}$ antibodies (1/1000 dilution in PBS; Merck Millipore, cat. no. AB1531). The specificity of the $GABA_BR$ antibodies has been described previously (Gassmann *et al.* 2004; Lacey *et al.* 2005), and the results of staining being specific to the use of the primary antibodies was demonstrated by omitting them during the staining procedures. After rinses in PBS, the sections were incubated for 16–18 h with gold (1.4 nm)-conjugated goat anti-guinea pig IgG antibodies (Nanoprobes Inc., Stony Brook, NY, USA) diluted 1/100 in PBS, and then, after further rinses in PBS, they were postfixed for 10 min with 2% glutaraldehyde in 0.1 M PB, followed by silver enhancement of the gold particles with an HQ Silver kit (Nanoprobes Inc.). The sections were then treated with 1% osmium tetraoxide in 0.1 M PB, dehydrated in a graded series of ethanol, and flat embedded on glass slides in Durcupan (Fluka) resin. Serial ultrathin sections (60 nm) of the LC region were cut and collected on single-slot copper grids coated with 1.5% Formvar in chloroform, stained with uranyl acetate followed by lead citrate, and examined on a JOEL JEM-2000 EXII electron microscope.

Synaptic structures were identified by the presence of a restricted zone of parallel pre- and postsynaptic membrane specializations with slight enlargement of the intercellular space, i.e. a visible synaptic cleft, and/or associated postsynaptic thickening, and by the accumulation of synaptic vesicles in the presynaptic profile (Peters *et al.* 1991). Synaptic junctions were classified as asymmetrical when a prominent plaque of dense material was seen on the cytoplasmic face of the postsynaptic membrane and as symmetrical when a less prominent density was seen on the postsynaptic membrane (Peters *et al.* 1991).

Results

Recording from LC neurons

In all electrophysiology experiments except the developmental study and the CTM treatment study, animals were killed for slice preparation on postnatal day (PN) 8–10. On a Nomarski microscopy video at low magnification, the LC was identified as a transparent, long, oval-shaped area located rostral to the floor of the 4th ventricle and beneath the superior cerebellar peduncle (Fig. 1*Aa–c*). At high magnification, numerous large neurons with a soma diameter of ~25 μm could be identified for recording (Fig. 1*Ad*). Initially, we filled the recorded neurons with biocytin to confirm that

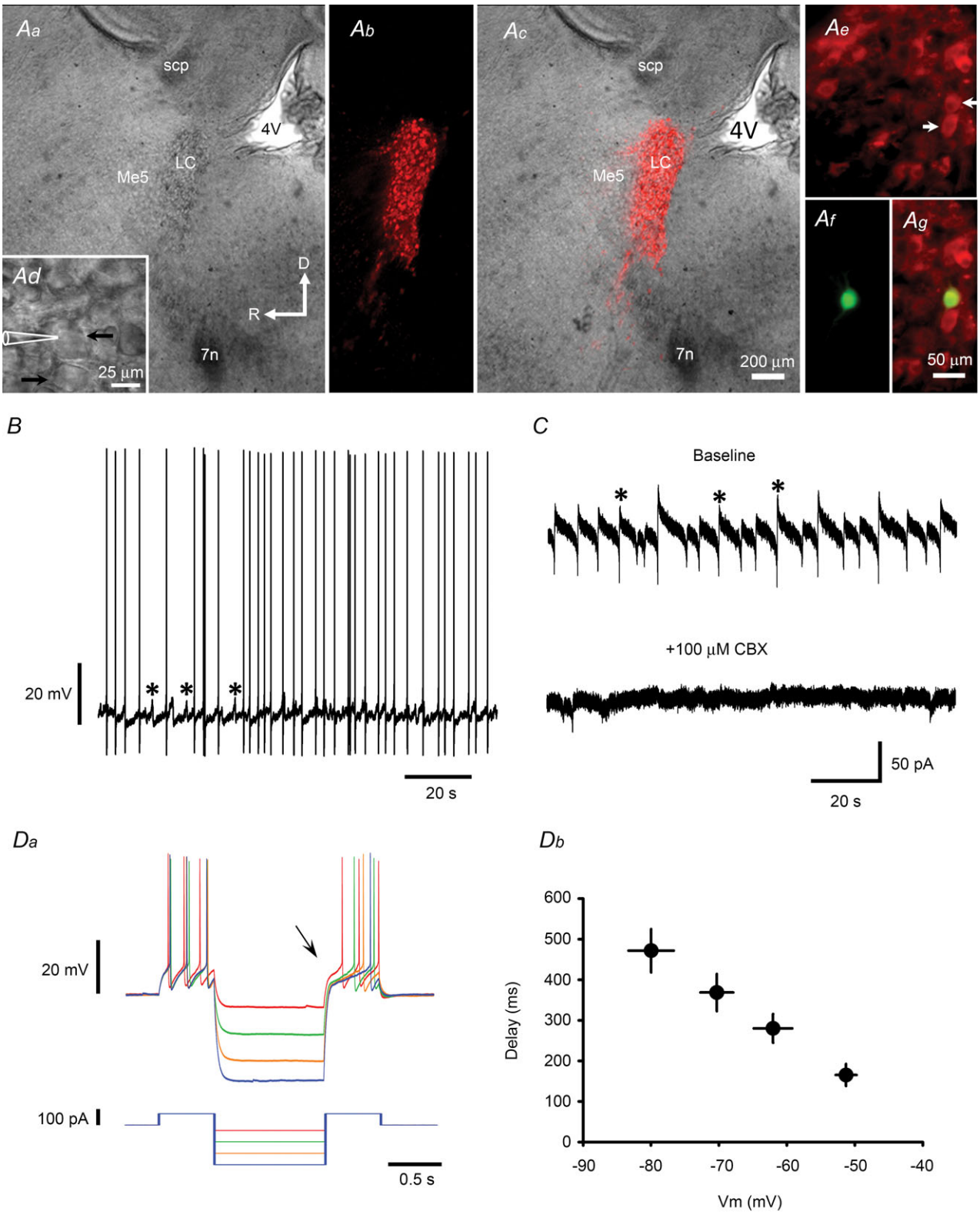

Figure 1. Recordings from LC neurons
A, identification of LC neurons in a sagittal brainstem slice. *Aa* and *Ad* are bright field images showing a paraformaldehyde-fixed slice at low magnification (*Aa*) and a non-fixed slice at high magnification (*Ad*). *Ab* and *Ac* are fluorescence images of slices stained with anti-TH antibody alone (*Ab*) or the merged image for *Aa* and *Ab* (*Ac*). Note the dense TH-ir neurons in the LC. *Ae–g* are fluorescence images of slices stained with anti-TH

these cells were immunoreactive (ir) with anti-TH antibody (Fig. 1*Ae–g*), but found that almost all were TH-ir and discontinued this practice when we started making cell-attached recordings. A feature of the current-clamp recordings from these TH-ir neurons was that the cells were able to spontaneously fire APs at ∼0.3 Hz and these were usually associated with membrane-voltage oscillations at 3.5 ± 0.7 Hz (asterisks in Fig. 1*B*). In voltage-clamp recordings, these events appeared as repeating biphasic currents (see asterisks in the upper trace in Fig. 1*C*) at the same frequency as the voltage oscillations seen in the current-clamp recordings and were blocked by CBX, a gap junction blocker (Fig. 1*C*). As it has been shown that neurons in the LC are electrically coupled (Ishimatsu & Williams, 1996; Ballantyne *et al.* 2004), these events could be due to the flow of AP currents through gap junctions. As seen previously in recordings from other pontine NA neurons (Min *et al.* 2008, 2010), on injection of hyperpolarizing current pulses, the TH-ir neurons in the LC showed a delay in the firing of APs, the duration of which was voltage dependent (Fig. 1*Da* and *b*), possibly caused by A-type potassium currents (Burdakov & Ashcroft, 2002). Taking all these features together, we considered that the recorded TH-ir neurons were indeed LC neurons.

Functional extrasynaptic $GABA_B$ receptors on LC neurons

Having confirmed that we were recording from LC neurons, the activity of their $GABA_B$Rs was characterized. Using a potassium gluconate-containing pipette solution and blocking $GABA_A$Rs by addition to the bath of 20 μM BicmBr, a selective $GABA_A$R antagonist, an outward current was induced by bath application of 10 or 100 μM GABA (I_{GABA}) or baclofen (I_{Bac}), a selective $GABA_B$R agonist (Fig. 2*Aa*), and this was shown to be dose dependent (Fig. 2*Ab*). As shown in Fig. 2*B*, the I_{GABA} and I_{Bac} induced by 100 μM baclofen (left panels) or GABA (right panels) were blocked by subsequent addition to the bath of 10 μM CGP54626, a $GABA_B$R inverse agonist, or 1 mM Ba^{2+}, a G protein-coupled inwardly rectifying potassium (GIRK) channel blocker, showing that they were $GABA_B$R-mediated currents resulting from the opening of GIRKs. The EC_{50} and the maximum amplitude of the I_{GABA} were 9.55 μM and 75.36 ± 3.69 pA ($n = 8$ cells), respectively, while the corresponding values for the I_{Bac} were 9.18 μM and 78.93 ± 4.07 pA ($n = 8$ cells). Interestingly, CGP reduced I_{GABA} and I_{Bac} to a level below baseline (see asterisks in Fig. 2*B*), indicating basal tonic activation of $GABA_B$Rs in LC neurons (see below) .

We next examined whether $GABA_B$R–GIRK signalling could be evoked by extracellular stimulation. As shown in Fig. 2*C*, outward currents with slow kinetics, referred to as slow-IPSCs and measured by charge transfer, were evoked on delivery of a stimulating train consisting of five pulses at 50 Hz, and subsequent bath application of 10 μM CGP54626 reduced these to 42 ± 4% of the baseline value ($n = 4$ cells; $P < 0.01$, paired t test), showing that $GABA_B$Rs were responsible for 58 ± 4% of the slow-IPSCs (left panel in Fig. 2*Da*). LC neurons are hyperpolarized by an autoreceptor feedback mechanism mediated by α_2-adrenoreceptors (α_2ARs), which also couple to GIRK channels (William *et al.* 1985). Since both $GABA_B$Rs and α_2ARs are coupled to GIRK channels, we examined whether the slow-IPSCs of the $GABA_B$R-mediated component were occluded by α_2AR activation. As shown in Fig. 2*Cb*, application of 100 nM RX781094, an α_2AR antagonist, reduced the slow-IPSC to 70 ± 3% of the total slow-IPSCs of the baseline value ($n = 4$ cells; $P < 0.01$, paired t test), showing that α_2AR–GIRK signalling also contributed to the slow-IPSC, and subsequent application of 10 μM CGP54626 in the presence of RX781094 reduced the residual slow-IPSCs by 57 ± 3% ($n = 4$ cells; $P < 0.01$, paired t test; Fig. 2*Cb* and *Da*), showing that contribution of $GABA_B$Rs to slow-IPSCs in the presence of RX781094 was similar to that without RX781094 application (Fig. 2*Da*). These results show minor occlusion of $GABA_B$R-mediated activity by α_2AR-mediated activity and suggest that the majority of these two receptors couple to different populations of GIRK channels in LC neurons. Application of a combination of 10 μM (s)-SNAP5114, a selective GABA transporter 1 (GAT1) blocker, and 50 μM NNC711, a selective GAT2/3 blocker, resulted in a significant increase in the slow-IPSCs to 219.7 ± 18.6% of the baseline value (Fig. 2*Cc* and *Db*, $n = 8$ cells) and subsequent application

antibody (*Ae*) or biocytin (*Af*) and the merged images (*Ag*). The TH-ir neurons marked with white arrows in *Ae* are those marked with black arrows in *Ad*; the upper neuron was recorded and filled with biocytin (*Af* and *g*). Abbreviations: 4 V, 4th ventricle; 7n, 7th nerve; Me5, mesencephalic trigeminal nucleus; scp, superior cerebellar peduncle. The large arrows in *Aa* indicate slice orientation (D: dorsal; R: rostral) and the scale (200 μm). *B*, representative current recording from a TH-ir neuron showing spontaneous firing of APs and voltage oscillations (asterisks). *C*, voltage-clamp recordings from the same neuron as in *B* showing that the membrane currents underlying the voltage oscillations (asterisks in top trace) are blocked by application of 100 μM CBX, a gap junction blocker (bottom trace). *D*, representative current-clamp recording showing membrane voltage (V_m) responses (top trace) to the current injection protocol shown in the bottom trace (*Da*) and the summarized results (*Db*). Note that the delay in the onset of the action potential after the end of the hyperpolarizing current pulse (see arrow in *Da*) is V_m dependent (*Db*).

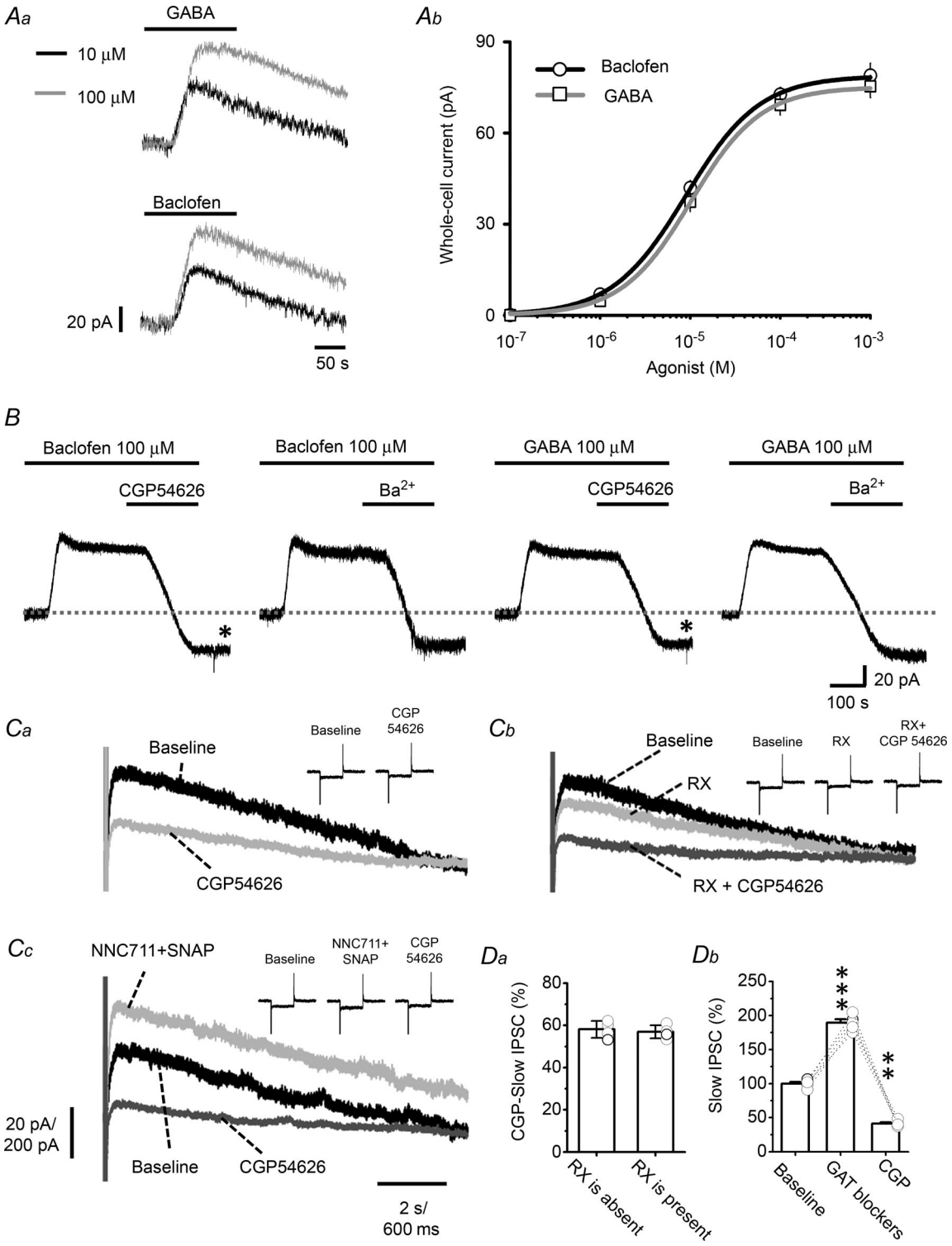

Figure 2. GABABR-GIRK currents in LC neurons
A, the traces in *Aa* are representative voltage-clamp recordings of the outward current induced by 10 or 100 μM baclofen or GABA. *Ab* shows summarized results using baclofen and GABA at concentrations of 0.1, 1, 10 and 100 μM and 1 mM and the fitting of the Hill equation to the data. *B*, representative recordings showing that the baclofen- or GABA-induced outward current is blocked by subsequent application of 10 μM CGP54626 or 1 mM Ba^{2+}. *C*, GABA$_B$R-mediated slow-IPSCs in LC neurons. *Ca*, superimposed representative recordings showing the slow-IPSCs evoked in LC neurons by a 5-pulse stimulating train at 50 Hz under baseline conditions and in

of CGP54626 in the presence of these GAT blockers dramatically reduced the slow-IPSCs to a level significantly below baseline (40.9 ± 4.9% of baseline, Fig. 2*Db*). These results show that the $GABA_BR$-mediated component of slow-IPSCs was enhanced by inhibition of GABA reuptake.

The dependence of the $GABA_BR$-mediated slow-IPSC on GABA reuptake suggests that it was mediated by $GABA_BRs$ at peri-/extrasynaptic sites. To confirm this, the subcellular distribution of $GABA_BRs$ was examined using a pre-embedding EM method. EM observations revealed that the GABA-ir gold particles were localized at the presynaptic terminals of both asymmetric (Fig. 3*Aa* and *d*) and symmetric (Fig. 3*Ac*) synapses. $GABA_BR$-ir gold particles were also found at the postsynaptic elements of these two types of synapse at both synaptic (Fig. 3*C*) and peri-/extrasynaptic sites (*Fig.* 3*A–C*). In addition, they were also found on the membrane of cytosolic organelles, some of which were located beneath the synaptic or perisynaptic active zone (Fig. 3*B*). Of the $GABA_BR$-ir gold particles found near synaptic structures, 39.8% were seen at presynaptic terminals (25% on the plasma membrane and 14.8% on the membranes of cytosolic organelles) and 60.2% at postsynaptic elements (24.2% on the plasma membrane and 36% on the membranes of cytosolic organelles). Of the 24.2% on the postsynaptic membrane, 0.8% were at synaptic sites, 5.4% at perisynaptic sites, and 18% at extrasynaptic sites. No $GABA_BR$-ir gold particles were seen in control sections in which primary antibody was omitted during staining (Fig. 3*D*). The EM observations show that most functional (surface) postsynaptic $GABA_BRs$ were at peri-/extrasynaptic sites, consistent with the slow-IPSC recording results (Fig. 2*Cc* and *Db*).

$GABA_BRs$, but not $GABA_ARs$, mediate tonic inhibition of LC neurons

The peri-/extrasynaptic location of $GABA_BRs$ on LC neurons suggested that they might be activated by ambient GABA and mediate tonic inhibition. We therefore tested whether a $GABA_BR$-mediated standing current was present in LC neurons. In line with the observation shown in Fig. 2*B*, application of 10 μM CGP54626 induced an inward current with an amplitude of 9.3 ± 0.3 pA ($n = 8$ cells) under conditions when $GABA_ARs$ were blocked, and similar results were obtained using another selective $GABA_BR$ inverse agonist, SCH50911 (20 μM) (inward current of 9.16 ± 0.43 pA, $n = 7$ cells) (Fig. 4*Aa* and *c*). We refer to this $GABA_BR$ antagonist-induced current as the $GABA_BR$-mediated standing current ($GABA_BR$-I_{Stand}) (see Wu *et al.* 2011). Since CGP54626 and SCH50911 both function as inverse agonists of $GABA_BRs$ (Grünewald *et al.* 2002), a neutral antagonist, CGP35348, was used to examine whether the $GABA_BR$-I_{Stand} resulted from activation of $GABA_BRs$ by ambient GABA or from constitutive activity of the receptor. Application of 100 μM CGP35348 induced a $GABA_BR$-I_{Stand} with a similar amplitude (9.1 ± 1.3 pA, $n = 4$ cells) to those induced by 10 μM CGP54626 or 20 μM SCH50911 (Fig. 4*Aa* and *c*). $GABA_BRs$ are shown to subject to allosteric modulation by Ca^{2+}, and Ca^{2+} concentrations in the physiological range can potentiate the ability of GABA to activate $GABA_BRs$ (Galvez *et al.* 2000). In LC neurons, the I_{GABA} induced by the application of 100 μM GABA in the absence of extracellular Ca^{2+} was 27.4 ± 8.6 pA ($n = 4$ cells) (Fig. 4*Ab*, top trace), corresponding to 34.7% of the amplitude induced in normal extracellular Ca^{2+} levels (2.5 mM) (see Fig. 2*Aa* and *b*), the difference between the two conditions being significant ($P < 0.001$, $F_{(1,11)} = 47.63$, one-way ANOVA test). The $GABA_BR$-I_{Stand} induced by 10 μM CGP54626 was also reduced (2.3 ± 1.3 pA; $n = 4$ cells) under Ca^{2+}-free conditions (Fig. 4*Ab* and *c*) to 24.7% of the amplitude under normal conditions (Fig. 4*Aa* and *c*) and, again, the difference was significant ($P < 0.001$, $F_{(1,11)} = 45.37$, one-way ANOVA test). These results show that $GABA_BRs$ on LC neurons are also subject to allosteric modulation by Ca^{2+}, and that the amplitude of the $GABA_BR$-I_{Stand} is dependent on GABA binding to $GABA_BRs$, i.e. was not due to constitutive activity of $GABA_BRs$. Like I_{GABA} and I_{Bac}, the induction of the $GABA_BR$-I_{Stand} by 10 μM CGP54626 failed (Fig. 4*B*) when GIRKs were blocked by the addition of 1 mM Ba^{2+} to the bath medium. Together, these results show that a $GABA_BR$-I_{Stand} of ∼10 pA peak, accounting for ∼13% of the maximal $GABA_BR$-mediated current (see dashed line in Fig. 4*C*), in LC neurons resulted from continuous

the presence of 10 μM CGP54626. *Cb* shows representative recordings of baseline, after addition of 100 nM RX781094 (RX), and after further addition of 10 μM CGP54626. *Cc* shows representative recording under baseline conditions after addition of two GAT blockers (50 μM NNC711 + 10 μM SNAP), and after further addition of 10 μM CGP54626. Inset traces in *Ca–c* show monitoring of series resistance by applying 5 mV voltage pulses throughout recording. Note no significant variance of series resistance. The vertical scale is 20 pA and 200 pA for recording of slow-IPSCs and series resistance monitoring, respectively, and the horizontal scale is 2 s and 600 ms for recording of slow-IPSCs and series resistance monitoring, respectively. *D*, summarized results of recording shown in *C*. *Da* shows the percentage blocking by CGP54626 of the slow-IPSCs (CGP slow-IPSC) in normal medium or the addition of the α2 blocker RX. *Db* shows the effect of GAT blockers on slow-IPSCs. The circles show results of individual experiments and the error bars show the mean and SEM for 4 cells (*Da*) or 8 cells (*Db*). The asterisks indicate a significant difference compared to the baseline value at the level of $P < 0.01$ (**) or $P < 0.001$ (***) using a paired *t* test. CGP, CGP54626.

activation of peri-/extrasynaptic $GABA_B$Rs by ambient GABA, rather than a constitutive activity of the receptors.

Since tonic inhibition mediated by extrasynaptic $GABA_A$Rs has been demonstrated in many CNS neurons (Farrant & Nusser, 2005), we examined whether this was also the case in LC neurons. Using a CsCl-based pipette solution and 1 μM TTX in the bath to block voltage-dependent Na^+ channels, many miniature IPSCs (mIPSCs) were seen, and these were blocked by subsequent application of 20 μM BicmBr (Fig. 4*Da*) or 20 μM GBZ (raw data not shown), showing that they were mediated by $GABA_A$Rs. Blockade of mIPSCs using BicmBr (Fig. 4*Da* and *Db*) or GBZ (Fig. 4*Db*) was not associated with a change in the holding current from baseline or the level of background noise (Fig. 4*Da*), indicating that there was only a minor, or no, $GABA_A$R-mediated tonic current. Together, these results show that the tonic inhibition of LC neurons is mediated by $GABA_B$Rs, and not $GABA_A$Rs.

Tonic inhibition can tune the SFR of LC neurons: role of GABA reuptake

The physiological role of $GABA_B$R tonic inhibition was next explored by examining its effect on the spontaneous firing rate (SFR) of LC neurons. To avoid a change in the intracellular ion composition, the cell-attached configuration was used. As with current-clamp recording (Fig 1*B*), LC neurons recorded using the cell-attached

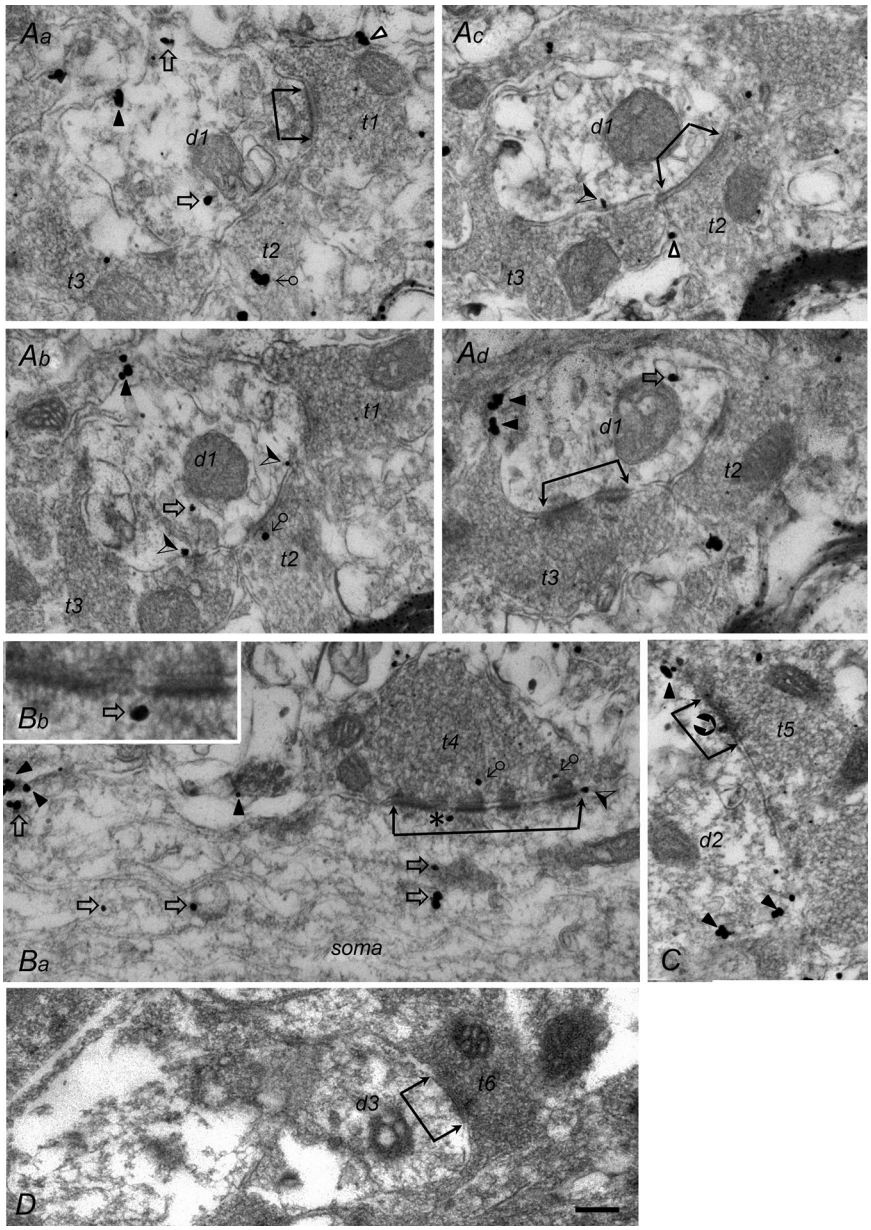

Figure 3. Subcellular distribution of $GABA_B$Rs in the LC
A, EM photographs of 4 serial ultrathin sections showing a dendrite (d1) receiving 3 axon terminals (t1–t3), with the contacts of the t1 and t3 terminal being asymmetric (*Aa* and *d*) and those of the t2 terminal (*Ac*) being symmetric. *B*, EM photograph showing an axon terminal (t4) making multiple asymmetric contacts with a soma at low (*Ba*) and high (*Bb*) magnification. *C*, EM photograph showing an axon terminal (t5) making symmetric contact on a dendrite (d2). *D*, EM photographs showing an axon terminal (t6) making asymmetric contact on a dendrite (d3) in a control section. All photographs, except that in *Bb*, are at the same magnification; the scale in *D* is 0.2 μm, which also applies to *A*, *Ba* and *C*; it indicates 0.08 μm for *Bb*. The active zones of the synaptic junctions are labelled with 2 connected arrows. $GABA_B$R-ir gold particles located on the plasma membrane of presynaptic terminals are indicated with the symbol Δ (*Aa* and *c*), those located on the membrane of cytosolic organelles in axonal terminals with ♂ (*Ab* and *Ba*), those located at the plasma membrane of the postsynaptic dendrite/soma with ▲ (extrasynaptic site; *Aa*, *b* and *d*, *Ba* and *C*), ⮝ (perisynaptic site; *Ab* and *Ba*), or ⬮ (synaptic site; see t5 in *C*), and those located on the membrane of cytosolic organelles in the dendrite/soma with ⇧ (*Aa*, *b* and *d*, *Ba* and *b*). Note that *Bb* shows part of the active zone t4 (indicated by the asterisk in *Ba*) at high magnification with a $GABA_B$R-ir gold particle on a cytosolic organelle located beneath the active zone.

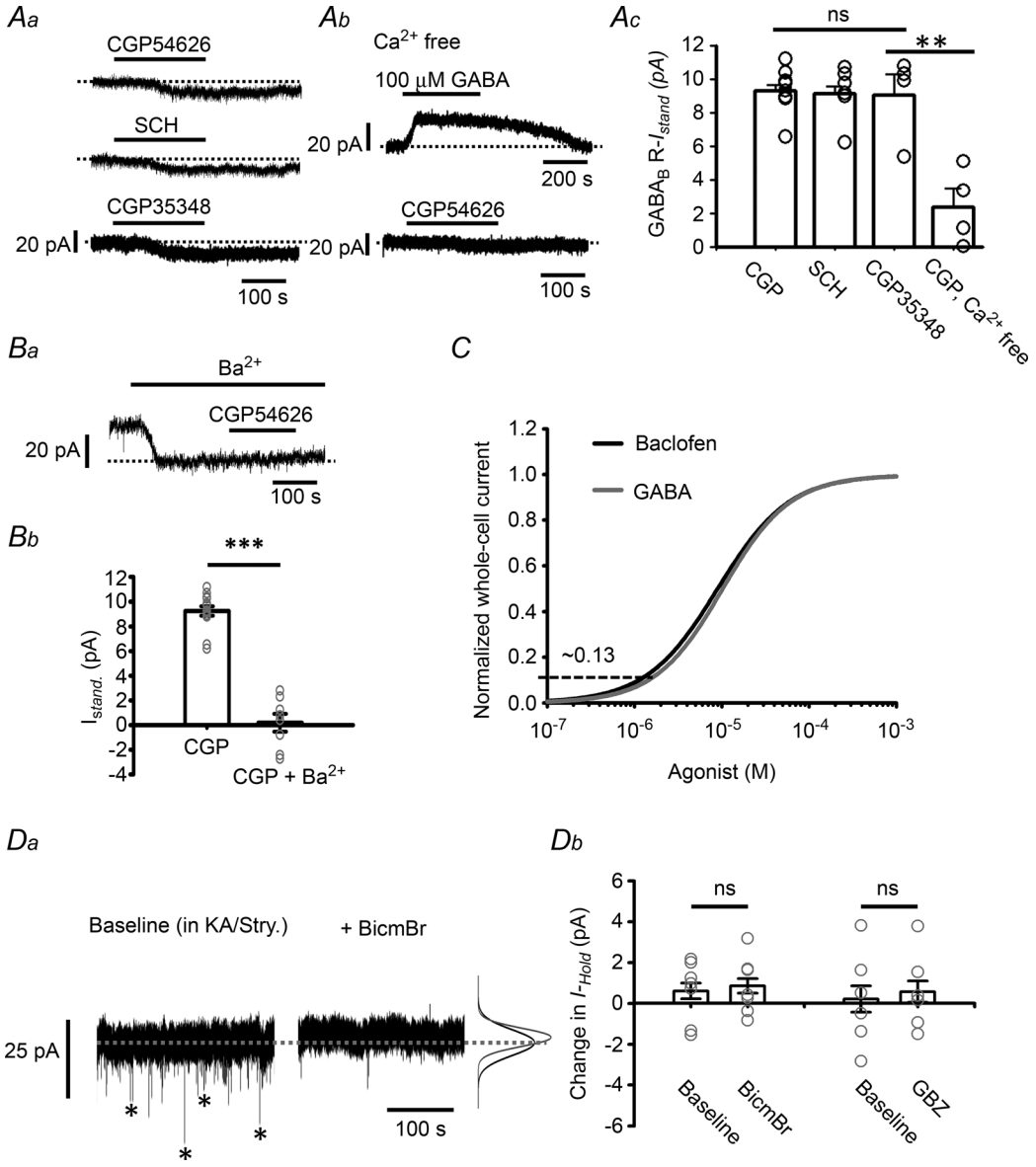

Figure 4. $GABA_BR$-I_{Stand} in LC neurons
A, representative recordings showing the $GABA_BR$-I_{Stand} induced by application of two inverse agonists, CGP54626 and SCH50911, and a neutral antagonist CGP35348 (*Aa*), the I_{GABA} induced by 100 μM GABA and the $GABA_BR$-I_{Stand} induced by 10 μM CGP54626 in Ca^{2+}-free medium (*Ab*), and the summarized results (*Ac*). CGP, CGP54626. *B*, induction of the $GABA_BR$-I_{Stand} by 10 μM CGP54626 in the presence of 1 mM Ba^{2+}; *Ba* shows a representative recording and *Bb* the summarized results compared to the values in the absence of Ba^{2+} (pooled data from CGP and SCH in panel *Ac*). *C*, normalization of the whole cell current *versus* concentration curve induced by GABA (grey) to that for baclofen (black) (data from Fig. 2*Ab*). The horizontal dashed line indicates the peak amplitude of the $GABA_BR$-I_{Stand}, which yields an estimate of the percentage of the $GABA_BR$-I_{Stand} to the $GABA_BR$-mediated total whole-cell current. *Da*, representative recordings of GABAergic mIPSCs (asterisks in the left trace), which are blocked by application of 20 μM BicmBr (right trace). Note that the inhibition of the mIPSC is not associated with a change in the holding current (dashed line) or noise level (indicated by the Gaussian curves on the right; black baseline, grey after BicmBr application). *Db*, summarized results for the effects of BicmBr and GBZ on the holding current. In all plots, the circles show results of individual experiments, while the error bars are the mean and SEM. ns in *Ac* and *Db* indicates no significant difference using one-way ANOVA or the paired *t* test, respectively, while ** in *Ac* and *** in *Bb* indicate, respectively, a statistically significant difference at the $P < 0.01$ and $P < 0.001$ level using Student's *t* test.

method showed an SFR of ∼0.3 Hz in the baseline recording (Fig. 5*Aa*, trace 1, and *b*), which was not affected by bath application of 20 μM BicmBr (Fig. 5*Aa*, trace 2, and *b*; $n = 10$ cells, paired *t* test, $P = 0.158$), but was significantly increased from 0.31 ± 0.02 to 0.72 ± 0.03 Hz by the addition of 10 μM CGP54626 (Fig. 5*Aa*, trace 3, and *b*, paired *t* test, $P < 0.001$). In addition, increasing the extent of tonic inhibition by increasing ambient GABA levels to activate more peri-/extrasynaptic GABA$_B$Rs resulted in a significant decrease in the SFR of LC neurons. As shown in Fig. 5*B*, after a stable period of baseline recording (Fig. 5*Ba*, trace 1, and *b*), bath application of a combination of 50 μM NNC711 and 10 μM (s)-SNAP5114 to inhibit GABA reuptake resulted in a dramatic decrease in the SFR from 0.27 ± 0.02 Hz to 0.11 ± 0.01 Hz (Fig. 5*Ba*, trace 2 and *b*, $n = 8$ cells; $P < 0.001$, paired *t* test) and, while subsequent application of BicmBr had no effect (Fig. 5*Ba*, trace 3 and *b*), application of CGP54626 not only reversed the effect of the GAT1/2 blockers, but also increased the SFR to 0.38 ± 0.02 Hz (Fig. 5*Ba*, trace 4, and *b*, $P < 0.001$, paired *t* test, compared to baseline). In summary, these results show that varying the extent of GABA$_B$R tonic inhibition can effectively tune the SFR of LC neurons. Interestingly, there was no significant effect of BicmBr application on the SFR even when GABA reuptake was blocked (Fig. 5*B*). These results show that no GABA$_A$R-mediated tonic inhibition was seen in LC neurons.

An increase in GABA$_B$R activity increases tonic inhibition and maintains the SFR of LC neurons constant in developing rats

In addition to ambient GABA levels, the effect of manipulating GABA$_B$R activity on the tonic inhibition and thus the SFR of LC neurons was also tested. Postnatal

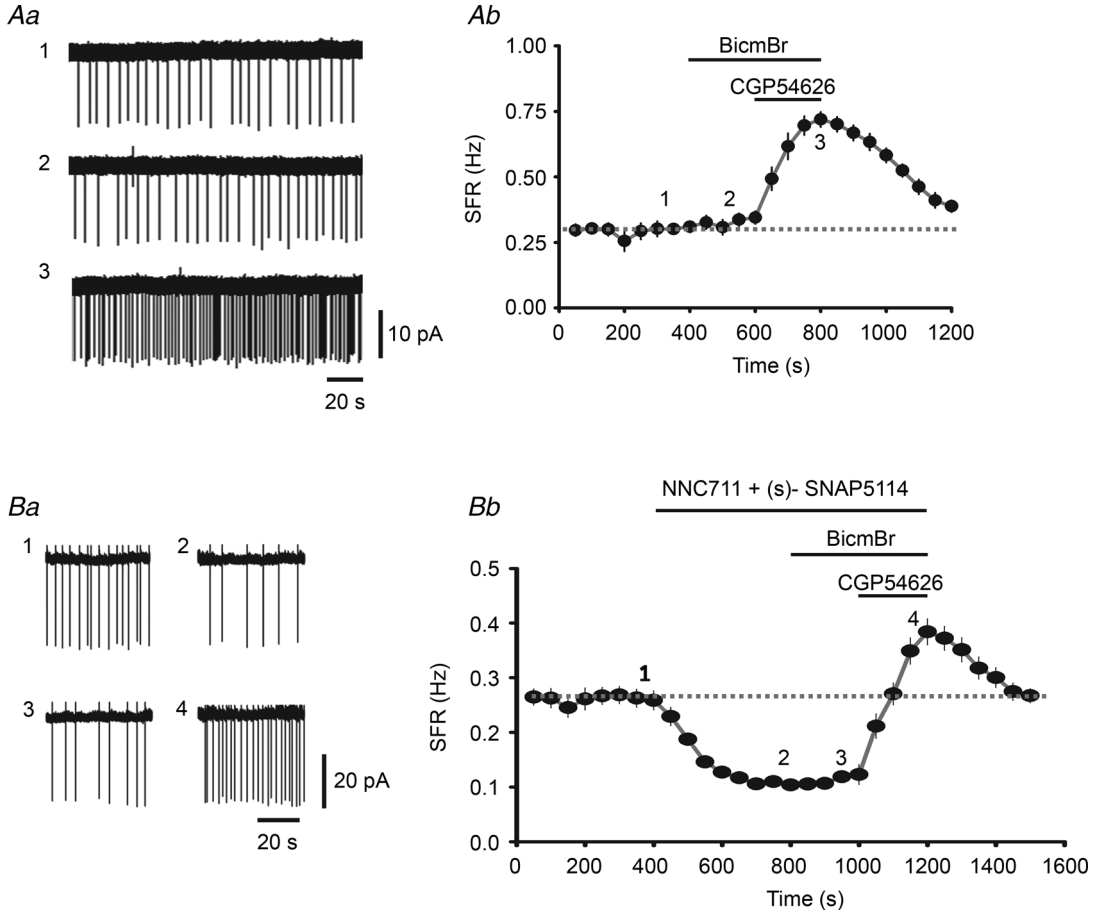

Figure 5. Tonic inhibition tunes the SFR of LC neurons and the effect of GABA reuptake
A, representative cell-attached recordings of the SFR of an LC neuron (*Aa*) at the times indicated by 1, 2 and 3 in the summarized results (*Ab*) showing the entire time-course of the recordings. Note the baseline SFR (trace 1) is not affected by 20 μM BicmBr (trace 2), but is dramatically increased by 10 μM CGP54626 (trace 3). In *Ab*, each point (circle plus vertical line) represents the mean and SEM for the instant firing rate averaged over a recording period of 50 s. *B*, representative recordings (*Ba*) and summarized results (*Bb*) showing the effect of prior application of the GAT1 blocker NNC711 (50 μM) and the GAT2/3 blocker (s)-SNAP5114 (10 μM).

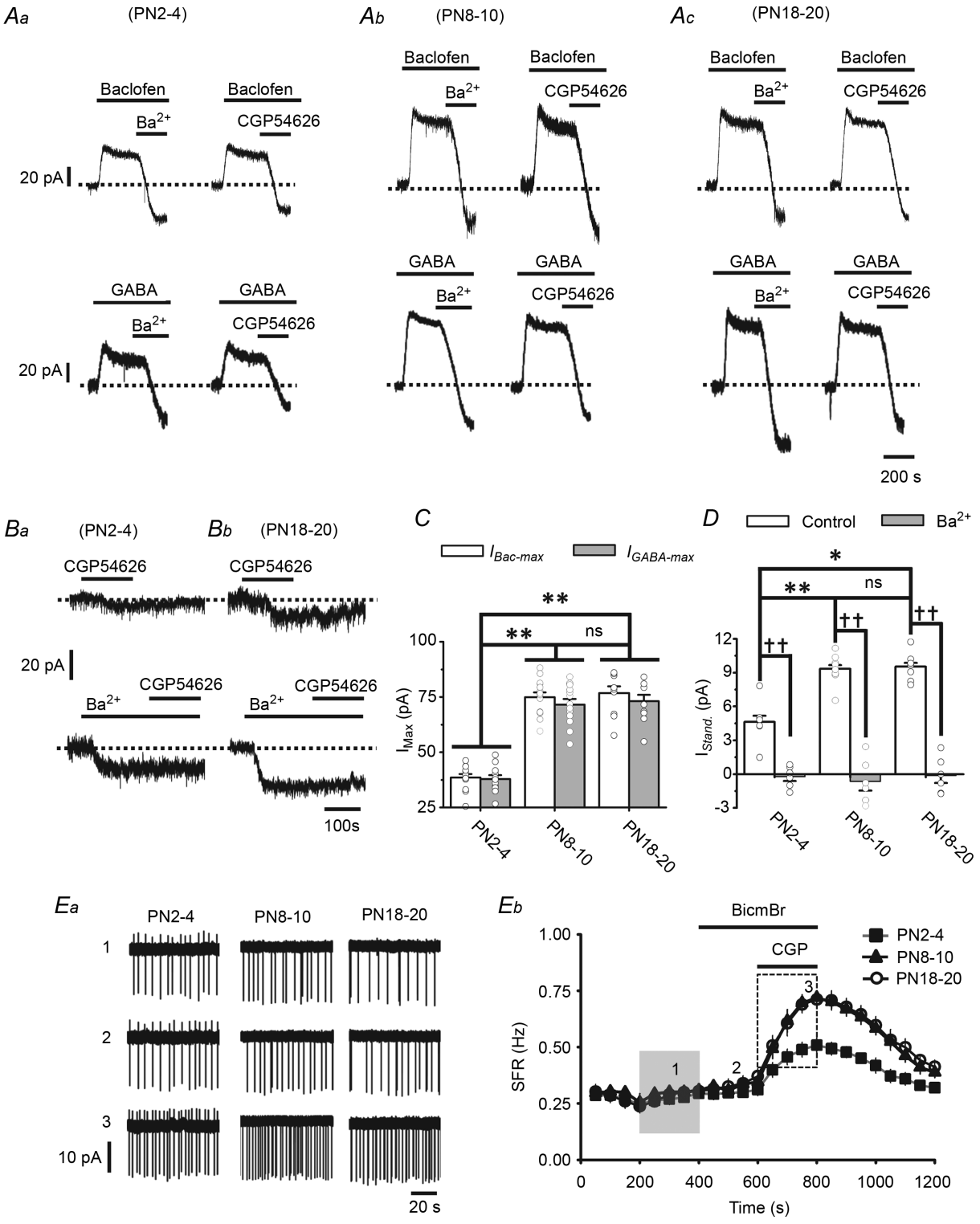

Figure 6. Increased $GABA_BR$ activity in LC neurons enhances tonic inhibition: developmental study
A, representative recordings showing the $I_{Bac\text{-}Max}$ (upper traces) and $I_{GABA\text{-}Max}$ (lower traces) induced by 1 mM baclofen and 1 mM GABA, respectively, in LC neurons in slices prepared at PN2–4 (*Aa*), PN8–10 (*Ab*), or PN18–20 (*Ac*). Note that the $I_{Bac\text{-}Max}$ and $I_{GABA\text{-}Max}$ are blocked by subsequent application of 1 mM Ba^{2+} or 10 μM CGP54626. *B*, representative recordings showing the $GABA_BR$-I_{Stand} induced by 10 μM CGP54626 under normal conditions (upper traces) and in the presence of 1 mM Ba^{2+} (lower traces) in slices taken at PN2–4 (*Ba*) or PN18–20 (*Bb*). *C* and *D*, summarized results showing the developmental increase in the $I_{Bac\text{-}Max}$ and $I_{GABA\text{-}Max}$ (*C*) and the $GABA_BR$-I_{Stand}

development was used as the study model to examine the effect of increasing GABA$_B$R activity. In addition to PN8–10, two additional PN ages, PN2–4 and PN18–20, were examined. As shown in *Fig.* 6*A* and *C*, on going from PN2–4 to PN8–10, an increase in the maximal I_{Bac} ($I_{Bac\text{-}Max}$) and I_{GABA} ($I_{GABA\text{-}Max}$) induced by 1 mM baclofen or 1 mM GABA was seen in LC neurons. The peak amplitudes of the $I_{Bac\text{-}Max}$ and $I_{GABA\text{-}Max}$ were, respectively, 40.8 ± 2.2 pA ($n = 7$ cells) and 39.8 ± 2.7 pA ($n = 7$ cells) at PN2–4 and 79.2 ± 3.6 pA ($n = 8$ cells) and 78.9 ± 4.1 pA ($n = 8$ cells) at PN8–10 (Fig. 6*Aa* and *b*, and *C*; one-way ANOVA, $P < 0.01$, $F_{(1,14)} = 42.65$ for Bac, $F_{(1,14)} = 39.56$ for GABA); the $I_{Bac\text{-}Max}$ and $I_{GABA\text{-}Max}$ at PN18–20 did not differ from those induced at PN8–10 (Fig. 6*Ab* and *c*, and *C*; one-way ANOVA, $P = 0.971$, $F_{(1,15)} = 0.02$ for Bac, $P = 0.864$, $F_{(1,15)} = 0.03$ for GABA). Consistent with the lower $I_{Bac\text{-}Max}$ and $I_{GABA\text{-}Max}$ seen at PN2–4, as shown in Fig. 6*B* and *D*, the GABA$_B$R-I_{Stand} recorded at PN2–4 was 4.6 ± 0.8 pA ($n = 8$ cells), significantly lower than that recorded at PN8–10 (9.2 ± 0.4 pA, $n = 15$ cells, $P < 0.01$, $F_{(1,22)} = 27.05$, one-way ANOVA) or PN18–20 (9.5 ± 0.5 pA, $n = 8$ cells, $P < 0.05$, $F_{(1,15)} = 11.46$, one-way ANOVA). Induction of the GABA$_B$R-I_{Stand} was blocked at all developmental stages when CGP or Ba^{2+} was added to the bath (Fig. 6*B* and *D*). Interestingly, no significant difference in the baseline SFR was observed among the three developmental stages (~0.25 Hz, shaded area in Fig. 6*Eb*) unless the GABA$_B$R-I_{Stand} was abolished by addition of CGP54626 to the bath (dashed area in Fig. 6*Eb*). At all three developmental stages, the SFR was significantly increased after blockade of GABA$_B$Rs (Fig. 6*Ea* and *b*; $P < 0.001$ in all cases, paired *t* test), but the increase was significantly lower at PN2–4 than at PN8–10 or PN18–20. After removal of tonic inhibition, the SFR of LC neurons at PD2–4 was 0.51 ± 0.03 Hz ($n = 8$ cells), significantly lower than that of 0.72 ± 0.03 Hz at PN8–10 ($n = 10$ cells, $P < 0.01$, $F_{(1,17)} = 18.31$, one-way ANOVA) and that of 0.71 ± 0.03 Hz at PN18–20 ($n = 8$ cells, $P < 0.01$, $F_{(1,17)} = 16.85$, one-way ANOVA) (Fig. 6*Ea* and *b*). There was no difference in the resting V_m (measured with addition to the bath of 1 μM TTX) among the three groups (PN2–4: 45.2 ± 2.3 mV, $n = 10$ cells; PN8–10: 45.4 ± 2.1 mV, $n = 12$ cells; PN18–20: 44.9 ± 2.7 mV, $n = 10$ cells; $P = 0.99$, $F_{(2,31)} = 0.01$, one-way ANOVA). These results show that, during development, the GABA$_B$R-I_{Stand} and tonic inhibition increase to maintain the SFR of LC neurons at a constant level of 0.3 Hz. As already seen for the PN8–10 stage (*Fig.* 5*A* and *B*), BicmBr had no effect on the SFR at the other developmental stages (Fig. 6*E*).

A decrease in GABA$_B$R functionality caused by chronic perinatal citalopram treatment inhibits tonic inhibition and results in abnormal SFRs of LC neurons

In addition to increasing GABA$_B$R activity and tonic inhibition, the functional outcome of a manipulation reducing these parameters was also investigated. In dorsal raphe neurons, a prolonged increase in serotonin agonist levels caused either by knockdown of the serotonin transporter (Mannoury la Cour *et al.* 2001) or by chronic treatment with an SSRI (fluoxetine) leads to reduced levels of somatodendritic GABA$_B$Rs (Cornelisse *et al.* 2007). We therefore examined whether a similar downregulation of GABA$_B$R activity also occurred in LC neurons after chronic SSRI treatment and, if so, what effect it had on tonic inhibition. The model described by Darling *et al.* (2011) was used; male and female rats were injected subcutaneously with the SSRI CTM (10 mg (kg body weight)$^{-1}$) or 0.9% NaCl twice a day from PN5 to PN12 and measurements were made at PN18–20. As shown in Fig. 7 (see also Table 1), the $I_{Bac\text{-}Max}$ was significantly reduced by 28.3 ± 4.7% in CTM-treated male rats compared to saline-treated male rats (*Fig.* 7*A* and *C*; $n = 6$ cells, $P < 0.01$, $F_{(1,23)} = 12.84$, two-way ANOVA) and the $I_{GABA\text{-}Max}$ was significantly reduced by 26.6 ± 5.4% ($n = 6$ cells, $P < 0.01$, $F_{(1,23)} = 14.68$, two-way ANOVA) (*Fig.* 7*A* and *D*), but no effect was seen in female rats (Fig. 7*B–D*; Table 1). In addition, there was no difference between the $I_{Bac\text{-}Max}$ and $I_{GABA\text{-}Max}$ recorded in LC neurons of saline-treated male or CTM-treated female rats (Fig. 7*B–D*; Table 1). Consistent with the reduction in the $I_{Bac\text{-}Max}$ and $I_{GABA\text{-}Max}$, the GABA$_B$R-I_{Stand} was significantly decreased in CTM-treated male rats compared to saline-treated male rats (29.5 ± 6.2%, $n = 16$ cells, $P < 0.01$, $F_{(1,41)} = 16.02$, two-way ANOVA), but no effect was seen in female rats (Fig. 7*E* and *F*; Table 1). There was no difference in the resting V_m (measured with addition to the bath of 1 μM TTX) between the male

(*D*). ∗ and ∗∗ indicate $P < 0.05$ or < 0.01, respectively, between different developmental groups using one-way ANOVA, and ns indicates no significant difference between the indicated groups using the same test. †† indicates a difference at the level of $P < 0.01$ between the Ba^{2+} group and control group within a developmental stage using Student's *t* test. *Ea*, representative recording from an LC neuron at different developmental stages showing the SFR at baseline (trace 1) and after application of 20 μM BicmBr (trace 2) followed by 10 μM CGP54626 (trace 3) at the time points indicated in *Eb*. *Eb*, summarized results showing the entire time-course of the recordings for all 3 developmental stages. Note there is no difference in baseline SFR among the three developmental groups (shaded rectangle) and that, after CGP application, the SFR is significantly lower at PN2–4 than the other developmental stages (dashed rectangle).

and female groups or between treatment groups (two-way ANOVA, $P = 0.57$, $F_{(1,24)} = 1.25$, see Table 1). These results show that CTM treatment results in reduced $GABA_BR$ activity in LC neurons in male, but not female, rats.

In slices from CTM-treated male rats, the baseline SFR of the LC neurons was 0.56 ± 0.01 Hz ($n = 6$ cells), significantly higher than that of 0.29 ± 0.02 Hz in slices from saline-treated male rats ($n = 6$ cells; $P < 0.001$, $F_{(1,23)} = 37.51$, two-way ANOVA) (compare traces 1 and 1′ in Fig. 8*Aa* and the dashed rectangle in Fig. 8*B*; Table 1). In contrast, there was no difference in the baseline SFR between CTM-treated and saline-treated female

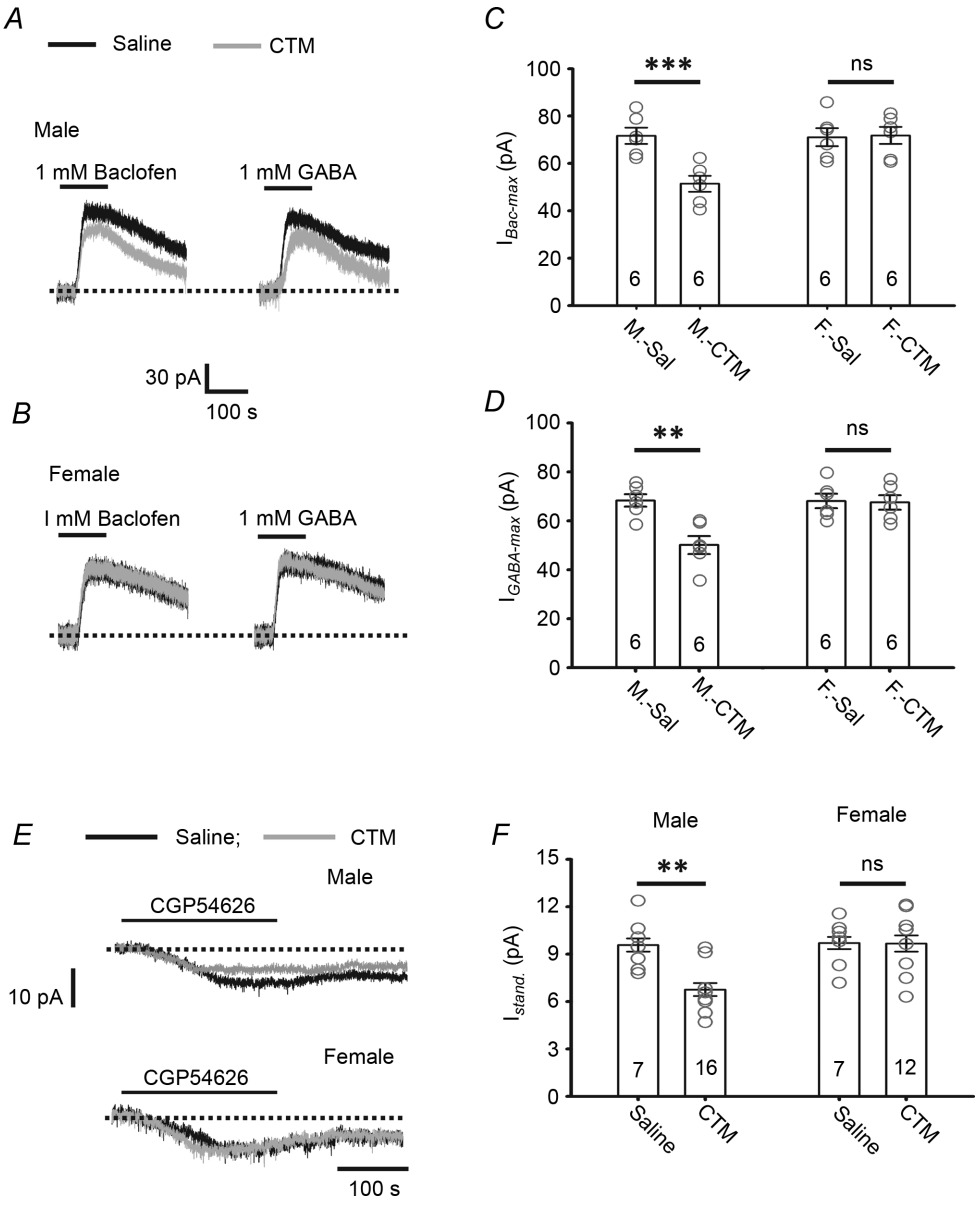

Figure 7. Chronic perinatal CTM exposure reduces $GABA_BR$ activity on LC neurons in male, but not female, rats

A–D, representative recordings showing the $I_{Bac\text{-}Max}$ and $I_{GABA\text{-}Max}$ induced in LC neurons by 1 mM baclofen or 1 mM GABA in CTM- or saline-treated male (*A*) or female (*B*) rats, and the summarized results for the $I_{Bac\text{-}Max}$ (*C*) and the $I_{GABA\text{-}Max}$ (*D*). *E* and *F*, representative recordings showing the $GABA_BR$-I_{Stand} induced by 10 μM CGP54626 in LC neurons from CTM-treated and saline-treated male rats and female rats (*E*) and the summarized results (*F*). In *C*, *D* and *F*, the circles are the results of individual experiments, while the error bars are the mean and SEM; the number of cells tested is indicated in each column. ** indicates a difference between the CTM-treated male rats (M-CTM) and saline-treated male rats (M-Sal) group at the level of $P < 0.01$ using two-way repeated-observation ANOVA. ns indicates no significant differences between the CTM-treated female rats (F-CTM) and saline-treated female rats (F-Sal) or between the M-Sal and F-Sal groups using the same test.

Table 1. Effect of chronic perinatal CTM exposure on the GABABRs on LC neurons

	Male		Female	
	Saline	CTM	Saline	CTM
Resting V_m (mV)	44.9 ± 2.3 ($n = 6$)	39.2 ± 2.4 ($n = 7$)	45.1 ± 2.4 ($n = 6$)	45.6 ± 2.6 ($n = 6$)
$I_{GABA\text{-}Max}$ (pA)	71.7 ± 3.4 ($n = 6$)	57.4 ± 3.2† ($n = 6$)	71.1 ± 3.8 ($n = 6$)	71.8 ± 3.6 ($n = 6$)
$I_{Bac\text{-}Max}$ (pA)	68.3 ± 2.5 ($n = 6$)	55.3 ± 3.0† ($n = 6$)	68.1 ± 3.0 ($n = 6$)	67.5 ± 3.0 ($n = 6$)
GABA$_B$R-I_{Stand} (pA)	9.6 ± 0.6 ($n = 7$)	7.0 ± 0.6† ($n = 16$)	9.7 ± 0.6 ($n = 7$)	9. 7 ± 0.7 ($n = 12$)
SFR-baseline (Hz)	0.32 ± 0.02 ($n = 6$)	0.59 ± 0.04† ($n = 6$)	0.31 ± 0.07 ($n = 6$)	0.31 ± 0.01 ($n = 6$)
SFR-BicmBr (Hz)	0.34 ± 0.03* ($n = 6$)	0.60 ± 0.03$^{\dagger ns}$ ($n = 6$)	0.33 ± 0.02^{ns} ($n = 6$)	0.35 ± 0.03^{ns} ($n = 6$)
SFR-CGP (Hz)	0.71 ± 0.05* ($n = 6$)	1.04 ± 0.06$^{\dagger *}$ ($n = 6$)	0.70 ± 0.04* ($n = 6$)	0.71 ± 0.02* ($n = 6$)

†Significant difference at $P < 0.01$ level compared to Male-CTM group using two-way repeated-observation ANOVA. Compared to SFR-baseline group * indicates significant difference at $P < 0.01$ level and ^{ns} indicates no significant difference, using paired t test.

rats (compare traces 1 and 1′ in Fig. 8*C* and the dashed rectangle in Fig. 8*D*; Table 1). Could the decrease in the $I_{Bac\text{-}Max}$ and $I_{GABA\text{-}Max}$ (activity of the GABA$_B$R) and the GABA$_B$R-I_{Stand} (tonic inhibition) caused by chronic perinatal CTM exposure result in the increased SFR of LC neurons seen in CTM-treated male rats? Support for this idea was obtained when removal of the GABA$_B$R-I_{Stand} by addition of CGP54626 to the bath reduced the difference in the SFR of LC neurons between CTM-treated and saline-treated male rats. As shown in Fig. 8, application of CGP54626 resulted in a significant increase in the SFR in all cases, regardless of sex or CTM treatment ($P < 0.001$ in all cases, paired t test; Table 1). However, the ratio of the baseline SFR recorded in saline-treated male rats to that in CTM-treated male rats was 1.84 and decreased to 1.46 after blockade of the GABA$_B$R-I_{Stand} (tonic inhibition), while that in females was ∼1 before and after application of CGP54626. Together, these results show that, in male rats subjected to chronic perinatal CTM exposure, there is less GABA$_B$R activity in LC neurons, and thus a lower GABA$_B$R-I_{Stand} and tonic inhibition, than in saline-treated rats. This lower GABA$_B$R functionality might partially account for the higher SFR of LC neurons seen in the CTM-treated male rats. Again, we did not observe any effect of BicmBr on the SFR (Fig. 8), regardless of sex or whether the animals received CTM or not. These results show that chronic perinatal CTM exposure does not alter the expression of extrasynaptic GABA$_A$Rs on LC neurons.

Finally, we examined whether the reduced GABA$_B$R activity in CTM-treated male rats involved a decrease in surface GABA$_B$Rs levels using a pre-embedding EM method. At stage PN20, 89 synapses were randomly sampled from three saline-treated and 89 from three CTM-treated male rats. There was no difference between the two groups in the pattern of surface GABA$_B$R distribution on postsynaptic membranes (*Fig.* 9*A* and *B*). As observed in the saline-treated group (*Fig.* 9*A*) and naive animals (Fig. 3), GABA$_B$R-ir gold particles were also found at postsynaptic locations at synaptic and peri- and extrasynaptic sites in the CTM-treated group (Fig. 9*B*). The density of GABA$_B$Rs, expressed as the number of GABA$_B$R-ir gold particles per 1 μm length of dendritic membrane is much higher at extrasynaptic sites than at peri- and synaptic sites ($P < 0.001$, $F_{(1,177)} = 88.48$, one-way ANOVA; Fig. 9*C*). For all three types of postsynaptic location, no difference in GABA$_B$R density was observed between the saline-treated and CTM-treated group ($P = 0.85$, $F_{(1,177)} = 0.61$, two-way ANOVA; Fig. 9*C*). These results show that the reduction in GABA$_B$R activity in LC neurons from CTM-treated male rats did not involve a decrease in surface GABA$_B$R expression.

Discussion

Our argument for GABA$_B$R-mediated tonic inhibition of LC neurons is based on the observations that bath application of two different GABA$_B$R inverse agonists, CGP54626 and SCH50911, and a neutral antagonist, CGP35348, induced an inward standing current (GABA$_B$R-I_{Stand}) and increased the SFR in LC neurons. Since all three GABA$_B$R blockers produced the same results and since the induction of the GABA$_B$R-I_{Stand} was abolished by blockade of GIRK, a well-known effector molecule downstream of GABA$_B$R activation,

the $GABA_BR$-mediated tonic inhibition of LC neurons was a specific, rather than a non-specific, effect of these drugs. In addition, as CGP35348, one of the drugs used, is a neutral antagonist and since the induction of the $GABA_BR$-I_{Stand} by CGP54626 (an inverse agonist) is seen at an extracellular calcium concentration in the physiological range (2.5 mM), but not in Ca^{2+}-free medium, the tonic inhibition is mainly caused by activation of $GABA_BRs$ by ambient GABA and is not a constitutive activity of the receptor.

Previous EM studies showed that, in all brain regions examined, most $GABA_BRs$ are located at peri- and/or extrasynaptic sites, rather than synaptic sites (Boyes & Bolam, 2003; Kulik *et al.* 2003; Lacey, 2005), and an electrophysiology study showed that activation of these extrasynaptic $GABA_BRs$ is critically dependent on GABA reuptake and increases when GABA transporters are blocked (Beenhakker & Huguenard, 2010). The activation of $GABA_BRs$ on LC neurons is consistent with these features, as our EM results showed that very few $GABA_BR$-ir gold particles in postsynaptic locations were located at synaptic and perisynaptic sites and most were located at extrasynaptic sites; in addition, our electrophysiological studies showed a critical dependence of the activation of these extrasynaptic $GABA_BRs$ on GABA uptake, as the $GABA_BR$-mediated slow-IPSCs and tonic inhibition were dramatically increased by blockade of GABA reuptake. The time course of $GABA_BR$-mediated slow-IPSCs in the present study is much slower than those reported in previous studies (Beenhakker & Huguenard,

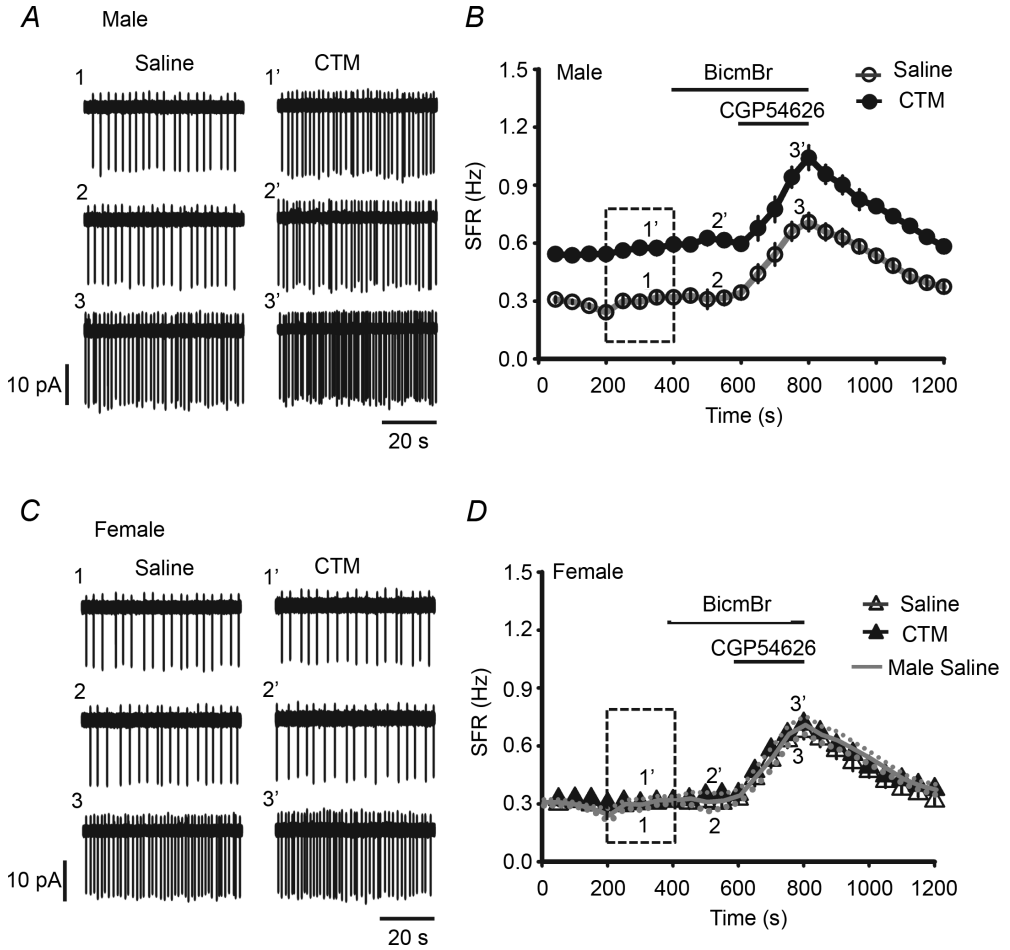

Figure 8. A reduction in $GABA_BR$ activity on LC neurons decreases tonic inhibition: chronic perinatal CTM exposure study
A, representative recordings from an LC neuron in a saline-treated male rat (1–3) and a CTM-treated male rat (1′–3′) showing the SFR at baseline (traces 1 and 1′) and after application of 20 μM BicmBr (traces 2 and 2′) followed by 10 μM CGP54626 (traces 3 and 3′); the numbers refer to the times in the time-course shown in *B*. *B*, summarized results showing the entire time-course of the recordings. Note the significant difference in the baseline SFR between the saline- and CTM-treated groups (dashed rectangle). *C* and *D*, representative recordings in saline- or CTM-treated female rats (*C*) and the summarized results (black lines and symbols) (*D*). Note CTM has no effect on the baseline SFR (dashed rectangle). The continuous and dotted lines (grey) in *D* are the results (mean ± SEM) for the saline-treated male rats taken from panel *B* and superimposed for comparison.

2010). An explanation for this could be that there is a unique distribution pattern and activity of GABA transporters in the LC that results in an ambient GABA profile generating a slow GABA$_B$R-mediated response following electrical stimulation. In addition to GABA$_B$R, the evoked slow-IPSCs also contain an α_2AR-mediated response with the α_2AR-mediated component being smaller than that of GABA$_B$R. However, using stimulation parameters similar to the present study, Courtney & Ford (2014) report a robust α_2AR-mediated IPSC in LC neurons. Since Kimura & Nakamura (1987) report that, although α_2ARs already function in LC neurons at birth, the activation of these autoreceptors by NA released from the synaptic terminals does not occur until PN9 and becomes mature in PN24–34, the discrepancy between Courtney & Ford's results and ours regarding the amount of α_2AR-mediated IPSC evoked in LC neurons might be due to the use of different ages of animals for brain slice preparation. Courtney & Ford (2014) used Sprague–Dawley rats aged 3–6 weeks, while PN8–10 rats of the same strain were used in the present study for recording slow-IPSCs. In addition, α_2AR-mediated whole-cell current induced in LC neurons of PN8–10 rats by addition into the bath of 50 μM UK14304, a selective α_2AR agonist, is 41.2 ± 7.1 pA ($n = 6$ cells; raw data not shown), which is smaller than GABA$_B$R-mediated current and further explains a smaller contribution of α_2AR-mediated response to the slow-IPSCs. Although extrasynaptic GABA$_A$Rs have been reported to be present in many brain regions examined (Farrant & Nusser, 2005; Glykys & Mody, 2007*a*,*b*; Belelli *et al.* 2009), they do not seem to play a role in mediating GABA tonic inhibition in LC neurons (also see Belujon *et al.* 2009), as no difference was seen in the holding current or the SFR when GABA$_A$Rs was blocked in the normal condition or in the condition in which GABA reuptake by GATs was inhibited.

In addition to ambient GABA levels, tonic inhibition also varied with GABA$_B$R activity on LC neurons. We observed a developmental increase in GABA$_B$R activity on LC neurons and, consistent with this, an increase in both the GABA$_B$R-I_{Stand} and tonic inhibition. It has been reported that, in the cortex of neonatal rats, GABA$_B$R-mediated somatic responses to baclofen application increase until the middle of the second postnatal week, and then remain stable (Luhmann & Prince, 1991; for review see Le Magueresse & Monyer, 2013). The present results are in agreement with this observation, as the I_{Bac} and I_{GABA} of LC neurons did not change after PN8–10. Interestingly, there was no significant difference in the SFR of LC neurons among the three developmental ages examined (see also Nakamura *et al.* 1987) unless GABA$_B$R-mediated tonic inhibition was blocked. It is possible that there is a developmental increase in the number of ion channels that are involved in generating spontaneous APs in LC neurons and that their function is counteracted by increased GABA$_B$R-mediated tonic inhibition, resulting in a constant level of SFR of LC neurons during postnatal developmental. The physiological significance of maintaining a constant SFR during development remains to be explored. Since NA plays many important roles in regulating development and cortical plasticity (Lipton & Kater, 1989; Kasamatsu, 1991) and since it has been suggested that abnormal behaviours could result from developmental dysregulation of the LC–NA system (for review see Mehler & Purpura, 2009), the maintenance of a stable SFR of LC neurons might ensure suitable ambient NA levels for the maturation of normal brain function.

SSRIs, including CTM, are preferred for antidepressant treatment because of their low toxicity and wide

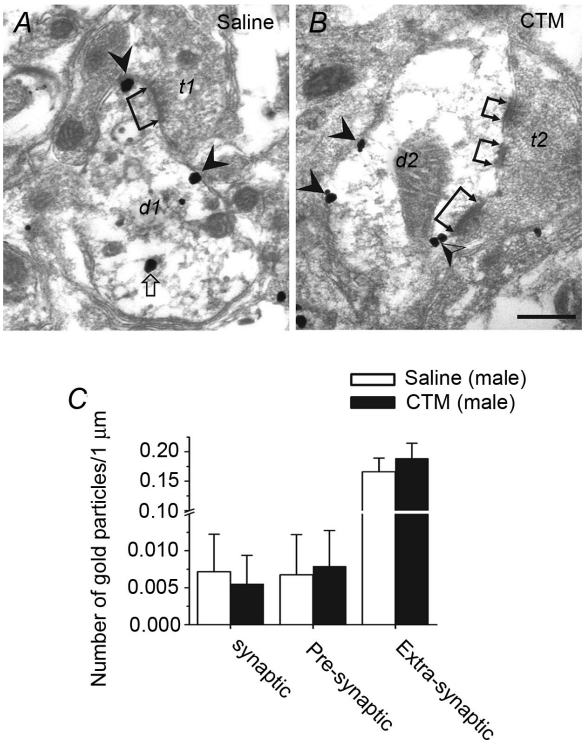

Figure 9. CTM treatment does not change the distribution and density of GABA$_B$Rs in the LC
A, EM photograph of a section from a saline-treated male rat showing an axon terminal (t1) making an asymmetric contact (see dual-headed arrow) on a dendrite (d1) in the LC. GABA$_B$R-ir gold particles can be seen at extrasynaptic sites (⮝) and on a cytosolic organelle (⇧). *B*, EM photographs of sections from CTM-treated male rats showing axon terminals (t2) making asymmetric contacts (dual-headed arrows) on a dendrite (d2) in the LC. GABA$_B$R-ir gold particles can be seen at extrasynaptic sites (⮝) and perisynaptic sites (⮝). *C*, distribution of GABA$_B$R-ir gold particles at synaptic sites, and perisynaptic and extrasynaptic sites in the LC at 89 synapses on slides prepared from 3 saline-treated or CTM-treated males. Note that most GABA$_B$R-ir gold particles are found at extrasynaptic sites in both the saline- and CTM-treated groups. The scale bar is 0.2 μm in *A* and *B*.

therapeutic index. The major pharmacological effect of SSRIs is inhibition of serotonin reuptake, increasing ambient serotonin levels. LC neurons are known to receive dense serotoninergic innervations from the dorsal raphe nucleus and pericoeruleus 5-HT neurons (Cedarbaum & Aghajanian, 1978; Aston-Jones *et al.* 1991; Kim *et al.* 2004) and their SFR has been shown to be modulated by serotonin (Haddjeri *et al.* 1997). Consistent with these facts, SSRI treatment has a profound effect on LC neuron activity. In mature rats, chronic SSRI exposure for 8–14 days leads to a reduction in the SFR of LC neurons (Nestler *et al.* 1990; Szabo *et al.* 1999; West *et al.* 2009). However, in contrast to these results, our results in juvenile rats and those of Darling *et al.* (2011) in mature rats show an increase in the SFR of LC neurons in male, but not female, rats receiving chronic perinatal CTM treatment. Although the cellular mechanisms underlying this observation remain to be explored, the present results are the first to show that downregulation of $GABA_BR$–GIRK activity and, thus, of tonic inhibition is involved.

In dorsal raphe neurons, both 5-HT_{1A} receptor (5-HT_{1A}R)- and $GABA_BR$-induced GIRK currents are reduced in rats after chronic treatment with fluoxetine, another SSRI (Cornelisse *et al.* 2007). Since 5-HT_{1A}Rs and $GABA_B$Rs are coupled to the same population of GIRKs (Innis *et al.* 1987; Williams *et al.* 1988), and since there is a parallel reduction in 5-HT_{1A}R–GIRK and $GABA_BR$–GIRK currents (Cornelisse *et al.* 2007), it has been previously proposed that GIRKs, rather than 5-HT_{1A}Rs and $GABA_B$Rs, are desensitized after chronic fluoxetine exposure. In support of this, radioligand-binding results have shown that GIRKs, but not 5-HT_{1A}Rs, are desensitized after chronic fluoxetine exposure (Pejchal *et al.* 2002; Shen *et al.* 2002; Castro *et al.* 2003). In line with these observations, our EM study showed that chronic perinatal CTM exposure did not alter the distribution and density of $GABA_B$Rs on the postsynaptic membrane in the LC, showing that the reduced $GABA_BR$–GIRK activity could not be ascribed to a decrease in surface $GABA_B$Rs, but may be due to the GIRK desensitization described above and/or other mechanisms, such as change in $GABA_BR$ phosphorylation, $GABA_BR$–GIRK coupling efficiency, regulators of G-protein signalling protein activity, and activity of the auxiliary $GABA_B$ receptor subunit, K^+ channel tetramerization domain-containing protein (for review, see Padgett & Slesinger, 2010; Gassmann & Bettler, 2012).

In summary, our studies of chronic perinatal CTM exposure, development, and inhibition of GABA reuptake (activity of GATs) clearly showed that alteration of $GABA_BR$-mediated tonic inhibition can effectively tune the SFR of LC neurons and thus LC–NA-associated brain function. For example, since ambient GABA levels in the LC are significantly higher during REM/non-REM sleep than during wakefulness (Nitz & Siegel, 1997; Nelson *et al.* 2002), our results suggest that $GABA_BR$-mediated tonic inhibition may play an important role in regulating the SFR of LC neurons, and thus the wakefulness/arousal level of the brain. In addition to postsynaptic regulation, $GABA_B$Rs at presynaptic sites have been shown to regulate glutamate and GABA release in many brain areas (Wu *et al.* 2011; Wang *et al.* 2013), perhaps including the LC neurons, as our EM study showed presynaptic location of $GABA_B$Rs in the LC. As $GABA_BR$ signalling and the activity of GABA transporters in many physiological and pathological processes can be regulated by various transmitter/receptor systems, such as the activation of 5-HT_{1A} receptors during chronic exposure to SSRIs, our results suggest that tonic inhibition and presynaptic regulation of transmitter release mediated by peri/extrasynaptic $GABA_B$Rs on LC neurons could be important players in the development of normal and abnormal behaviours/brain functions that are associated with the LC–NA system.

References

Adams LM & Foote SL (1988). Effects of locally infused pharmacological agents on spontaneous and sensory-evoked activity of locus coeruleus neurons. *Brain Res Bull* **21**, 395–400.

Aston-Jones G & Cohen JD (2005). An integrative theory of locus coeruleus-norepinephrine function: adaptive gain and optimal performance. *Annu Rev Neurosci* **28**, 403–450.

Aston-Jones G, Shipley MT, Chouvet G, Ennis M, van Bockstaele E, Pieribone V, Shiekhattar R, Akaoka H, Drolet G, Astier B, Charléty P, Valentino RJ & Williams JT (1991). Afferent regulation of locus coeruleus neurons: anatomy, physiology and pharmacology. *Prog Brain Res* **88**, 47–75.

Ballantyne D, Andrzejewski M, Muckenhoff K & Scheid P (2004). Rhythms, synchrony and electrical coupling in the locus coeruleus. *Respir Physiol Neurobiol* **143**, 199–214.

Beenhakker MP & Huguenard JR (2010). Astrocytes as gatekeepers of $GABA_B$ receptor function. *J Neurosci* **30**, 15262–15276.

Belelli D, Harrison NL, Maguire J, Macdonald RL, Walker MC & Cope DW (2009). Extrasynaptic $GABA_A$ receptors: form, pharmacology, and function. *J Neurosci* **29**, 12757–12763.

Belujon P, Baufreton J, Grandoso L, Boué-Grabot E, Batten TF, Ugedo L, Garret M & Taupignon AI (2009). Inhibitory transmission in locus coeruleus neurons expressing $GABA_A$ receptor epsilon subunit has a number of unique properties. *J Neurophysiol* **102**, 2312–2325.

Berridge CW & Foote SL (1991). Effects of locus coeruleus activation on electroencephalographic activity in neocortex and hippocampus. *J Neurosci* **11**, 3135–3145.

Berridge CW, Schmeichel BE & Espana RA (2012). Noradrenergic modulation of wakefulness/arousal. *Sleep Med Rev* **16**, 187–197.

Boyes J & Bolam JP (2003). The subcellular localization of $GABA_B$ receptor subunits in the rat substantia nigra. *Eur J Neurosci* **18**, 3279–3293.

Burdakov D & Ashcroft FM (2002). Cholecystokinin tunes firng of an electrically distinct subset of arcuate nucleus neurons by activating A-type potassium channels. *J Neurosci* **22**, 6380–6387.

Castro M, Diaz A, del Olmo E & Pazos A (2003). Chronic fluoxetine induces opposite changes in G protein coupling at pre and postsynaptic 5-HT_{1A} receptors in rat brain. *Neuropharmacology* **44**, 93–101.

Cedarbaum JM & Aghajanian GK (1978). Afferent projections to the rat locus coeruleus as determined by a retrograde tracing technique. *J Comp Neurol* **178**, 1–16.

Cornelisse LN, Van der Harst JE, Lodder JC, Baarendse PJ, Timmerman AJ, Mansvelder HD, Spruijt BM & Brussaard AB (2007). Reduced 5-HT_{1A}- and $GABA_B$ receptor function in dorsal raphe neurons upon chronic fluoxetine treatment of socially stressed rats. *J Neurophysiol* **98**, 196–204.

Courtney NA & Ford CP (2014). The timing of dopamine- and noradrenaline-mediated transmission reflects underlying differences in the extent of spillover and pooling. *J Neurosci* **34**, 7645–7656.

Darling RD, Alzghoul L, Zhang J, Khatri N, Paul IA, Simpson KL & Lin RC (2011). Perinatal citalopram exposure selectively increases locus ceruleus circuit function in male rats. *J Neurosci* **31**, 16709–16715.

Farrant M & Nusser Z (2005). Variations on an inhibitory theme: phasic and tonic activation of $GABA_A$ receptors. *Nat Rev Neurosci* **6**, 215–229.

Galvez T, Urwyler S, Prezeau L, Mosbacher J, Joly C, Malitschek B, Heid J, Brabet I, Froestl W, Bettler B, Kaupmann K & Pin J-P (2000). Ca^{2+}-requirement for high affinity γ-aminobutyric acid (GABA) binding at $GABA_B$ receptors: involvement of serine 269 of the $GABA_B$R1 subunit. *Mol Pharmacol* **57**, 419–426.

Gassmann M & Bettler B (2012). Regulation of neuronal $GABA_B$ receptor functions by subunit composition. *Nat Rev Neurosci* **13**, 380–394.

Gassmann M, Shaban H, Vigot R, Sansig G, Haller C, Barbieri S, Humeau Y, Schuler V, Müller M, Kinzel B, Klebs K, Schmutz M, Froestl W, Heid J, Kelly PH, Gentry C, Jaton AL, Van der Putten H, Mombereau C, Lecourtier L, Mosbacher J, Cryan JF, Fritschy JM, Lüthi A, Kaupmann K & Bettler B (2004). Redistribution of $GABA_{B(1)}$ protein and atypical $GABA_B$ responses in $GABA_{B(2)}$-deficient mice. *J Neurosci* **24**, 6086–6097.

Glykys J & Mody I (2007*a*). Activation of $GABA_A$ receptors: views from outside the synaptic cleft. *Neuron* **56**, 763–770

Glykys J & Mody I (2007*b*). The main source of ambient GABA responsible for tonic inhibition in the mouse hippocampus. *J Physiol* **582**, 1163–1178.

Grünewald S, Schupp BJ, Ikeda SR, Kuner R, Steigerwald F, Kornau HC & Köhr G (2002). Importance of the γ-aminobutyric $acid_B$ receptor C-termini for G-protein coupling. *Mol Pharmacol* **61**, 1070–1080.

Haddjeri N, de Montigny C & Blier P (1997). Modulation of the firing activity of noradrenergic neurones in the rat locus coeruleus by the 5-hydroxtryptamine system. *Br J Pharmacol* **120**, 865–875.

Innis RB & Aghajanian GK (1987). Pertussis toxin blocks 5-HT_{1A} and $GABA_B$ receptor-mediated inhibition of serotonergic neurons. *Eur J Pharmacol* **143**, 195–204.

Ishimatsu M & Williams JT (1996). Synchronous activity in locus coeruleus results from dendritic interactions in pericoerulear regions. *J Neurosci* **16**, 5196–5204.

Kasamatsu T (1991). Adrenergic regulation of visuocortical plasticity: a role of the locus coeruleus system. *Prog Brain Res* **88**, 599–616.

Kim MA, Lee HS, Lee BY & Waterhouse BD (2004). Reciprocal connections between subdivisions of the dorsal raphe and the nuclear core of the locus coeruleus in the rat. *Brain Res* **1026**, 56–67.

Kimura F & Nakamura S (1987). Postnatal development of α-adrenoceptor-mediated autoinhibition in the locus coeruleus. *Brain Res* **432**, 21–26.

Kulik A, Vida I, Luján R, Haas CA, López-Bendito G, Shigemoto R & Frotscher M (2003). Subcellular localization of metabotropic $GABA_B$ receptor subunits $GABA_{B1a/b}$ and $GABA_{B2}$ in the rat hippocampus. *J Neurosci* **23**, 11026–11035.

Lacey CJ, Boyes J, Gerlach O, Chen L, Magill PJ & Bolam JP (2005). $GABA_B$ receptors at glutamatergic synapses in the rat striatum. *Neuroscience* **136**, 1083–1095.

Le Magueresse C & Monyer H (2013). GABAergic interneurons shape the functional maturation of the cortex. *Neuron* **77**, 388–405.

Lipton SA & Kater SB (1989). Neurotransmitter regulation of neuronal outgrowth, plasticity and survival. *Trends Neurosci* **12**, 265–270.

Lu J, Bjorkum AA, Xu M, Gaus SE, Shiromani PJ & Saper CB (2002). Selective activation of the extended ventrolateral preoptic nucleus during rapid eye movement sleep. *J Neurosci* **22**, 4568–4576.

Luhmann HJ & Prince DA (1991). Postnatal maturation of the GABAergic system in rat neocortex. *J Neurophysiol* **65**, 247–263.

Luppi PH, Gervasoni D, Verret L, Goutagny R, Peyron C, Salvert D, Leger L & Fort P (2006). Paradoxical (REM) sleep genesis: the switch from an aminergic-cholinergic to a GABAergic-glutamatergic hypothesis. *J Physiol Paris* **100**, 271–283.

Mannoury la Cour C, Boni C, Hanoun N, Lesch KP, Hamon M & Lanfumey L (2001). Functional consequences of 5-HT transporter gene disruption on 5-HT_{1a} receptor-mediated regulation of dorsal raphe and hippocampal cell activity. *J Neurosci* **21**, 2178–2185.

Mehler MF & Purpura DP (2009). Autism, fever, epigenetics and the locus coeruleus. *Brain Res Rev* **59**, 388–392.

Min MY, Wu YW, Shih PY, Lu HW, Lin CC, Wu Y, Li MJ & Yang HW (2008). Physiological and morphological properties of, and effect of substance P on, neurons in the A7 catecholamine cell group in rats. *Neuroscience* **153**, 1020–1033.

Min MY, Wu YW, Shih PY, Lu HW, Wu Y, Hsu CL, Li MJ & Yang HW (2010). Roles of A-type potassium currents in tuning spike frequency and integrating synaptic transmission in noradrenergic neurons of the A7 catecholamine cell group in rats. *Neuroscience* **168**, 633–645.

Nakamura S, Kimura F & Sakaguchi T (1987). Postnatal development of electrical activity in the locus ceruleus. *J Neurophysiol* **58**, 510–524.

Nelson LE, Guo TZ, Lu J, Saper CB, Franks NP & Maze M (2002). The sedative component of anesthesia is mediated by $GABA_A$ receptors in an endogenous sleep pathway. *Nat Neurosci* **5**, 979–984.

Nestler EJ, McMahon A, Sabban EL, Tallman JF & Duman RS (1990). Chronic antidepressant administration decreases the expression of tyrosine hydroxylase in the rat locus coeruleus. *Proc Natl Acad Sci U S A* **87**, 7522–7526.

Nitz D & Siegel JM (1997). GABA release in the locus coeruleus as a function of sleep/wake state. *Neuroscience* **78**, 795–801.

Padgett CL & Slesinger PA (2010). $GABA_B$ receptor coupling to G-proteins and ion channels. *Adv Pharmacol* **58**, 123–147.

Pejchal T, Foley MA, Kosofsky BE & Waeber C (2002). Chronic fluoxetine treatment selectively uncouples raphe 5-HT_{1A} receptors as measured by [^{35}S]-GTPγS autoradiography. *Br J Pharmacol* **135**, 1115–1122.

Peters A, Palay SL & Webster H (1991). *The Fine Structure of the Nervous System*. Oxford University Press, New York.

Pfeiffer A & Zhang W (2007). Postnatal development of $GABA_B$-receptor-mediated modulation of potassium currents in brainstem respiratory network of mouse. *Respir Physiol Neurobiol* **158**, 22–29.

Shen C, Li H & Meller E (2002). Repeated treatment with antidepressants differentially alters 5-HT_{1A} agonist-stimulated [^{35}S]GTPγS binding in rat brain regions. *Neuropharmacology* **42**, 1031–1038.

Somogyi J & Llewellyn-Smith IJ (2001). Patterns of colocalization of GABA, glutamate and glycine immunoreactivities in terminals that synapse on dendrites of noradrenergic neurons in rat locus coeruleus. *Eur J Neurosci* **14**, 219–228.

Szabo ST, de Montigny C & Blier P (1999). Modulation of noradrenergic neuronal firing by selective serotonin reuptake blockers. *Br J Pharmacol* **126**, 568–571.

Tully K & Bolshakov VY (2010). Emotional enhancement of memory: how norepinephrine enables synaptic plasticity. *Mol Brain* **3**, 15.

Wang HY, Min MY & Yang HW (2012). $GABA_B$ receptor-mediated tonic inhibition of locus coeruleus neurons in developing rats. Program No. 537.07. 2012 Neuroscience Meeting Planner. Society for Neuroscience, New Orleans, LA, USA. Online.

Wang Y, Neubauer FB, Luscher HR & Thurley K (2010). $GABA_B$ receptor-dependent modulation of network activity in the rat prefrontal cortex *in vitro*. *Eur J Neurosci* **31**, 1582–1594.

Wang T, Rusu SI, Hruskova B, Turecek R & Borst JG (2013). Modulation of synaptic depression of the calyx of Held synapse by $GABA_B$ receptors and spontaneous activity. *J Physiol* **591**, 4877–4894.

West CH, Ritchie JC, Boss-Williams KA & Weiss JM (2009). Antidepressant drugs with differing pharmacological actions decrease activity of locus coeruleus neurons. *Int J Neuropsychopharmacol* **12**, 627–641.

Williams JT, Colmers WF & Pan ZZ (1988). Voltage- and ligand-activated inwardly rectifying currents in dorsal raphe neurons *in vitro*. *J Neurosci* **8**, 3499–3506.

Williams JT, Henderson G & North RA (1985). Characterization of alpha 2-adrenoceptors which increase potassium conductance in rat locus coeruleus neurones. *Neuroscience* **14**, 95–101

Wu Y, Wang HY, Lin CC, Lu HC, Cheng SJ, Chen CC, Yang HW & Min MY (2011). $GABA_B$ receptor-mediated tonic inhibition of noradrenergic A7 neurons in the rat. *J Neurophysiol* **105**, 2715–2728.

Additional information

Competing interests

The authors have no competing interests to declare.

Author contributions

H-Y.W. collected and analysed the electrophysiology data, and Z.-C.K. and Y.-S.F. collected and analysed the EM data. R.-F.C., M.-Y.M. and H.-W.Y. conceived and designed the experiments and wrote the first draft of the paper. The electrophysiological experiments were performed at NTU and CSMU, and EM experiments were performed at CHMU and NYMU. All authors have contributed to the writing of this paper and have approved its final version.

Funding

This work was supported by grants NSC-98-2311-B-002-003 -MY3 (R.-F. Chen), NSC - 99-2321-B-002-039 (M.-Y. Min) and NSC- 100-2320-B-040-010-MY3 (H.-W. Yang) from the National Science Council, Taiwan.

Acknowledgements

We thank Miss Y.-Y. Yu for EM support.